Cell Reports

Article

Integration of genetic and chromatin modification data pinpoints autoimmune-specific remodeling of enhancer landscape in CD4$^+$ T cells

Graphical abstract

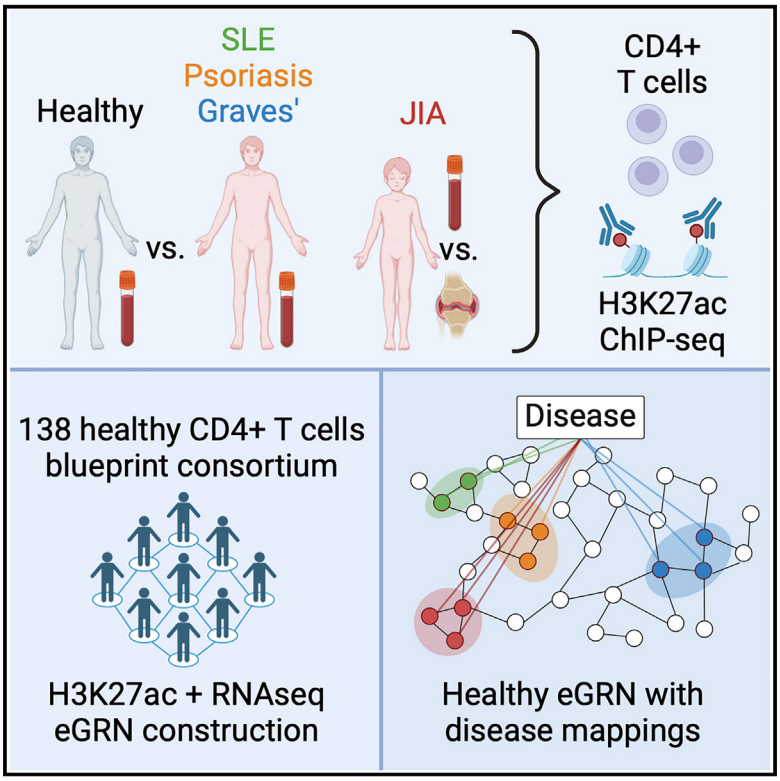

Authors

Neha Daga, Nila H. Servaas, Kai Kisand, ..., Pärt Peterson, Nikolina Nakic, Judith B. Zaugg

Correspondence

judith.zaugg@embl.de

In brief

Daga et al. investigate how gene regulatory mechanisms in CD4$^+$ T cells contribute to autoimmune disease. They integrate disease evidence from genetic associations and disease-specific enhancer and transcription factor activity via gene regulatory networks. The resulting disease-specific networks identify disease-relevant transcription factors and enhancers, which the authors validate with orthogonal data.

Highlights

- Enhancers and transcription factors in CD4 T cells show autoimmune-disease-specific activity
- Enhancer-mediated gene regulatory networks integrate divers types of disease evidence
- Disease-specific networks pinpoint disease-relevant enhancers and their target genes
- One disease-specific enhancer co-regulates *ICOS/CD28/CTL4A*, as validated by CRISPRi

Daga et al., 2024, Cell Reports *43*, 114810
October 22, 2024
https://doi.org/10.1016/j.celrep.2024.114810

CellPress

Cell Reports

CellPress
OPEN ACCESS

Article

Integration of genetic and chromatin modification data pinpoints autoimmune-specific remodeling of enhancer landscape in CD4$^+$ T cells

Neha Daga,[1,8] Nila H. Servaas,[1,8] Kai Kisand,[2] Dewi Moonen,[3] Christian Arnold,[1] Armando Reyes-Palomares,[1,9] Epp Kaleviste,[2] Külli Kingo,[4] Reet Kuuse,[5] Katrin Ulst,[5] Lars Steinmetz,[3,6] Pärt Peterson,[2] Nikolina Nakic,[7] and Judith B. Zaugg[1,8,10,*]

[1]Structural and Computational Biology Unit, European Molecular Biology Laboratory, Heidelberg, Germany
[2]Institute of Biomedicine and Translational Medicine, University of Tartu, Tartu, Estonia
[3]Genome Biology Unit, European Molecular Biology Laboratory, Heidelberg, Germany
[4]Department of Dermatology and Venerology, Faculty of Medicine, Institute of Clinical Medicine, University of Tartu, Tartu, Estonia and Dermatology Clinic, Tartu University Hospital, Tartu, Estonia
[5]Department of Internal Medicine, Tartu University Hospital, Tartu, Estonia
[6]Department of Genetics, Stanford University, Stanford, CA, USA
[7]Functional Genomics, Medicinal Science and Technology, GSK R&D, Stevenage, UK
[8]These authors contributed equally
[9]Present address: Department of Molecular Biology and Biochemistry, Faculty of Sciences, Andalucía Tech, University of Málaga, Málaga, Spain
[10]Lead contact
*Correspondence: judith.zaugg@embl.de
https://doi.org/10.1016/j.celrep.2024.114810

SUMMARY

CD4$^+$ T cells play a crucial role in adaptive immune responses and have been implicated in the pathogenesis of autoimmune diseases (ADs). Despite numerous studies, the molecular mechanisms underlying T cell dysregulation in ADs remain incompletely understood. Here, we used chromatin immunoprecipitation (ChIP)-sequencing of active chromatin and transcriptomic data from CD4$^+$ T cells of healthy donors and patients with systemic lupus erythematosus (SLE), psoriasis, juvenile idiopathic arthritis (JIA), and Graves' disease to investigate the role of enhancers in AD pathogenesis. By generating enhancer-based gene regulatory networks (eGRNs), we identified disease-specific dysregulated pathways and potential downstream target genes of enhancers harboring AD-associated single-nucleotide polymorphisms (SNPs), which we also validated using chromatin-capture (HiC) data and CRISPR interference (CRISPRi) in primary CD4$^+$ T cells. Our results suggest that alterations in the regulatory landscapes of CD4$^+$ T cells, including enhancers, contribute to the development of ADs and provide a basis for developing new therapeutic approaches.

INTRODUCTION

T cells play a central role in the initiation and regulation of adaptive immune responses. They fall into two main types: CD4$^+$ "helper" T cells (Th) and CD8$^+$ "cytotoxic" T cells. CD4$^+$ Th cells secrete cytokines that steer immune responses and activate innate immune cells, B cells, and CD8$^+$ T cells. Depending on the immunological trigger, CD4$^+$ T cells differentiate into one of five major Th cell subtypes with specialized functions[1] that are identified based on the secretion of specific cytokines and expression of lineage-specific transcription factors (TFs): Th1 (interferon [IFN]-γ and T-bet), Th2 (interleukin [IL]-4, IL-5, IL-13, and GATA3), T regulatory (Treg; IL-10, transforming growth factor [TGF]-β and FOXP3), Th17 (IL-17 and RORγT), and follicular T helper (Tfh, IL-21, and BCL6).[2] In addition, more controversial Th subsets include Th9 (IL-9 and SPI1)[3] and Th22 (IL-22 and AHR).[4] The tailored reactivity of these Th cell subsets is crucial for achieving effective adaptive immune responses.

Their critical role in orchestrating immune responses makes CD4$^+$ T cells important players in autoimmune disease (AD) pathogenesis: autoreactive CD4$^+$ T cells are implicated in systemic lupus erythematosus (SLE; a systemic AD causing widespread inflammation and organ damage),[5] psoriasis (characterized by chronic skin inflammation),[6] juvenile idiopathic arthritis (JIA; a rheumatic childhood disease causing local inflammation of the joints),[7] and Graves' disease (mainly affecting the thyroid gland).[8] The pathogenesis of these ADs has been linked with the dysregulation of specific Th subsets, including Tfh in SLE,[9] Th17 in psoriasis,[10] Treg in JIA,[11,12] and Th2 in Graves' disease.[13] However, the way in which these autoreactive T cells escape tolerance (i.e., unresponsiveness to self-antigens) and mediate autoimmunity is incompletely understood. Genetic susceptibility along with environmental triggers likely plays an

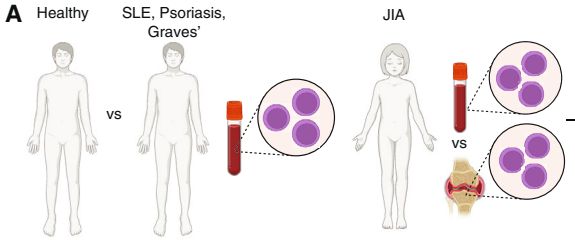

Disease	Donors	Sex	Tissue
SLE	Patient: 11 Healthy Control: 11	F: 11+11	PBMC
Psoriasis	Patient: 15 Healthy Control: 15	F: 7+7 M: 8+8	
Graves'	Patient: 13 Healthy Control: 10	F: 13+10	
JIA	Patient: 5 Patient Control: 3	F: 5	SF, PBMC

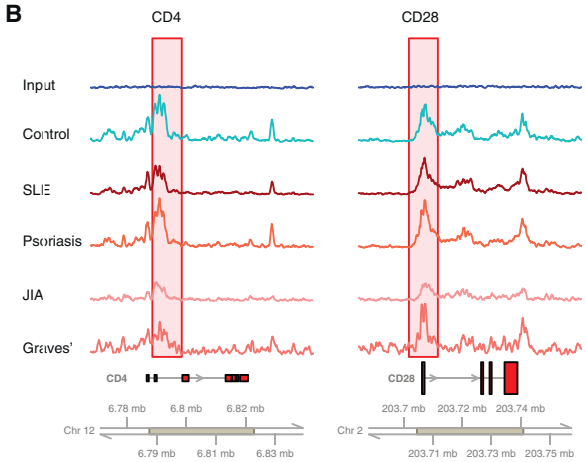

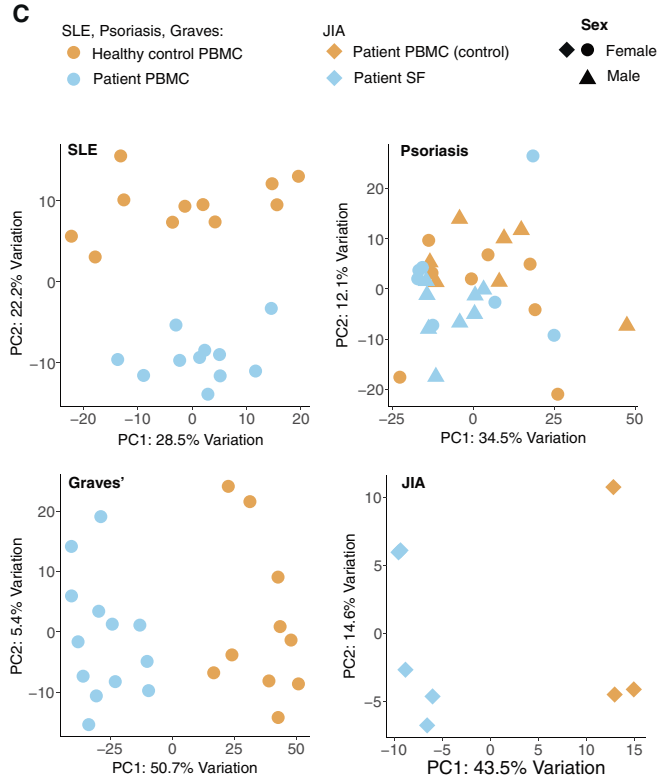

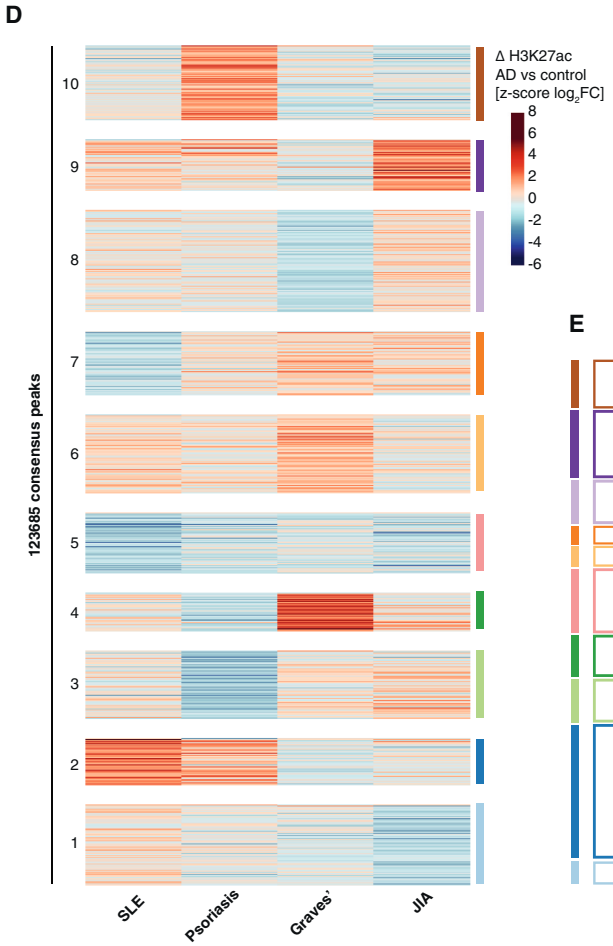

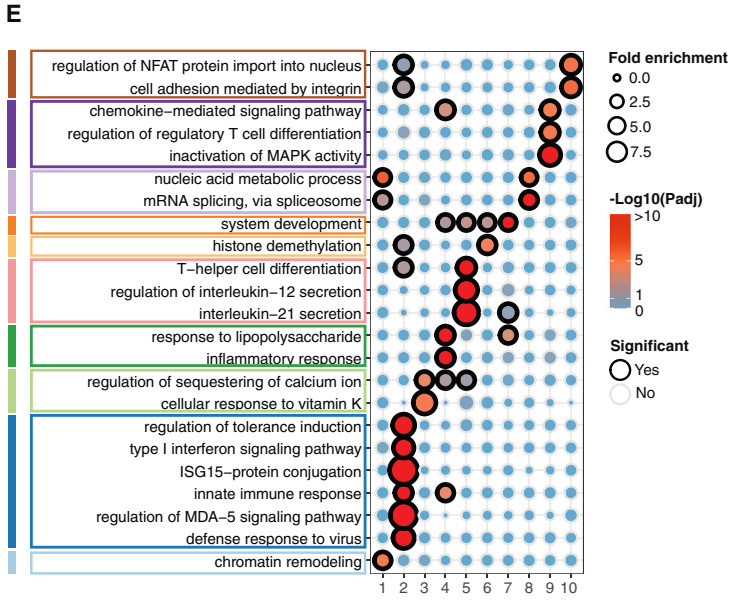

(legend on next page)

important role,[14] since many ADs have common genetic predispositions, including alterations in the human leukocyte antigen (HLA) region[15] (important for antigen presentation to T cells) and genes critical for T cell activation, including the IL-2 receptor (CD25), CTLA4, and PTPN22.[16] Yet, 90% of AD-associated single-nucleotide polymorphisms (SNPs) are located in the non-coding part of the genome,[17] suggesting that gene regulatory elements such as enhancers play an important role in disease manifestation. In line with this, Th subset differentiation is driven by TFs, and alterations at the epigenomic level, including histone modifications at enhancers, contribute to aberrant T cell activation in ADs.[18] However, for many AD-associated risk loci, we lack mechanistic insights into downstream target genes and how these contribute to a loss of T cell tolerance.

To address this, we studied the gene regulatory landscape, including enhancers and TFs, in CD4$^+$ T cells in SLE, psoriasis, JIA, and Graves' disease. We profiled enhancer and TF activities in patients and healthy controls using histone 3 lysin 27 acetylation (H3K27ac) chromatin immunoprecipitation followed by sequencing (ChIP-seq) and built a CD4$^+$ T cell-type-specific enhancer-based gene regulatory network (eGRN) to systematically integrate layers of molecular disease evidence, including disease-specific enhancer and TF activities and disease-associated genetic variants from genome-wide association studies (GWASs). Our approach of integrating molecular disease evidence using eGRNs identified disease-specific as well as common autoimmune pathways that are misregulated in AD pathogenesis, which we validated using CRISPR interference (CRISPRi) and chromatin interaction data. This study shows the power of eGRNs to uncover genes and their upstream regulators involved in ADs and may be utilized to prioritize genes for T cell-targeting treatments.

RESULTS

T cells in ADs show distinct H3K27ac changes between patients and controls

To investigate the role of enhancers in ADs, we performed H3K27ac ChIP-seq in CD4$^+$ T cells from peripheral blood mononuclear cells (PBMCs) of SLE (N = 11) and psoriasis (N = 15) patients at initial diagnosis along with age- and sex-matched healthy controls (N = 11 and N = 15 for SLE and psoriasis, respectively; Figure 1A). In addition, we obtained published H3K27ac data from CD4$^+$ T cells for Graves' disease and JIA. Specifically, we obtained data from Limbach et al., who profiled H3K27ac in PBMC-derived CD4$^+$ T cells in Graves' disease patients (N = 10) and age- and sex-matched healthy controls (N = 13),[19] and from Peeters et al., who profiled H3K27ac in CD4$^+$ T cells from synovial fluid (SF) of JIA patients and PBMCs of the same patients as controls (N = 5).[20] Due to the inaccessibility of healthy SF, we used SF-derived CD4$^+$ T cells from JIA patients as a proxy for local disease (N = 5) and PBMC-derived CD4$^+$ T cells from the same patients as controls (N = 3, a subset of the JIA cohort). This approach aligns with earlier studies on JIA.[11,20]

The H3K27ac data generated in this study for SLE and psoriasis was of high quality and showed the expected signal around promoter (transcription start site [TSS] ±3 kb) and enhancer regions (Figures S1A and S1B), and at the CD4 (a surface receptor highly expressed in CD4$^+$ T cells) and CD28 (an essential co-stimulatory molecule) loci, for all samples (Figure 1B). Peak calling per sample (STAR Methods) resulted in 107,897 (SLE), 126,308 (psoriasis), 71,298 (Graves' disease), and 26,730 (JIA) peaks. Principal-component analysis (PCA) based on the top 1,000 most variable H3K27ac peaks within each disease separated patients and controls in all diseases (Figure 1C), showing that the enhancer profiles of T cells in ADs are distinct from those of controls.

To compare the chromatin landscape across the different ADs, we generated a consensus H3K27ac peak set across the four diseases, resulting in 150,560 peaks (STAR Methods). Differential acetylation analysis for each disease-control setting revealed between 5 (psoriasis) and 18K (Graves' disease) differentially acetylated peaks (Figure S1C; Table S1). To get an unbiased view of the disease-specific enhancer profiles, we grouped the variable peaks (fold change >1 in at least one disease; 123,685 peaks) into 10 clusters based on their fold-change value using k-means clustering (Figure 1D). All clusters, except for cluster 5, showed disease-specific patterns. Cluster 5, which showed uniform downregulation in all diseases, is enriched in Gene Ontology (GO) terms related to Th differentiation (Figure 1E), in line with the important role of Th cells in ADs.[22] Cluster 9 (upregulated in three of the four diseases, most strongly in JIA), is enriched in chemokine signaling pathways, and regulation of Treg differentiation, likely reflecting the important role of Tregs in JIA and other ADs.[11,23] Psoriasis-specific cluster 10 is enriched in cell adhesion processes, in line with disease characteristics related to disturbed cellular adhesion that can contribute to T cell dysregulation in psoriatic skin.[24] Graves' disease-specific cluster 4 is enriched in general processes related to inflammatory responses, whereas SLE-upregulated cluster 2 is enriched in type I IFN signaling and defense response to viruses (important in SLE pathogenesis[25,26]). These results indicate that AD T cells are characterized by general and disease-specific enhancer signatures that potentially regulate disease-relevant biological pathways.

TF activity reveals shared and disease-specific inflammatory T cell processes across ADs

We previously demonstrated that changes in H3K27ac marks aggregated across TF binding sites can serve as a readout of

Figure 1. Identification of autoimmune-disease-specific H3K27ac profiles

(A) Schematic representation of CD4$^+$ T cell isolation and H3K27ac ChIP-seq from patients and controls; table containing sample information including the number of biological replicates (donors) for each disease (F, female; M, male).

(B) Genomic tracks with H3K27ac signal around CD4 and CD28 genes for representative samples.

(C) PCA based on top 1,000 most variable peaks within each disease cohort.

(D) k-means clustering of consensus peak set based on log2 fold changes in H3K27ac marks between patients and controls.

(E) GO enrichment terms for each cluster in (D) based on closest genes using GREAT (significant: adjusted $p \leq 0.1$).

differential TF activity, and we developed diffTF to facilitate this analysis.[27] Using diffTF, we identified 341 (Graves' disease), 189 (SLE), 263 (psoriasis), and 41 (JIA) differentially active TFs between patients and controls (Table S2). One hundred TFs are differentially active in at least three diseases (Figure 2A), with 12 TFs being commonly upregulated across all diseases (Figure 2B). These include members of the activating protein 1 (AP-1) complex (JUN and FOS) and the NF-κB complex (NFKB2 and TF65) that play important roles in T cell activation, a critical process generally dysregulated in autoimmune conditions.[28–30] We confirmed the expression of these TFs in PBMC-derived naive CD4$^+$ T cells from 138 healthy donors of the BLUEPRINT consortium using RNA sequencing (RNA-seq) (Figure S2A).

We found 186 TFs differentially active in only one disease. These include Th-lineage-defining TFs, such as RORG (essential for Th17[31]), AHR (Th22[32]), and TBX21 (Th1[33]) in psoriasis; the Tfh-specific TF BCL6[34,35] in SLE; and the Th9-specific TF SPI1[36] in Graves' disease (Figure 2C). These lineage-specific TFs are in line with previous studies that highlighted Th17, Th22, and Th1 in psoriasis[37,38]; Tfh in SLE[9,39]; and Th9 in Graves' disease.[40] Other disease-specific TFs suggest further dysregulation of signaling pathways in T cells: in SLE, IFN regulatory factors (IRF3, 5, 7, and 9) and STAT family members (STAT1 and STAT2) showed increased activity in patients (Figure 2D). The majority of these TFs were more highly expressed in SLE patients than in healthy controls based on analysis of publicly available RNA-seq data[41] of PBMC-derived CD4$^+$ T cells (Figure S2B). These TFs are involved in the aberrant expression of type I IFN genes, known as the "type I IFN signature," an important hallmark of SLE[25,26] and in line with the enriched GO terms in the SLE-dominated cluster 9 (Figure 1E). These observations confirm the findings of a previous study that compared TF activities inferred from RNA-seq data between SLE and healthy controls in a larger cohort.[42] In Graves' disease, the CAAT/enhancer-binding protein (C/EBP) TF family showed high activity (Figure 2E), consistent with its known association with inflammatory cytokines (IL-6, IL-1β, and tumor necrosis factor-α [TNF-α]) and its role in regulating macrophage and neutrophil functions.[43] In psoriasis, we observed high activity of KAISO, CREB1, and CREB5 (Figure 2F), implicated in the regulation of TGF-β signaling,[44–46] which plays a major role in psoriasis pathogenesis.[47] Indeed, single-cell RNA-seq data of CD45$^+$ immune cells from skin biopsies[48] showed significantly higher expression of KAISO and CREB1 in psoriatic patients than in healthy controls for most T cell populations in skin (Figure S2C). Last, members of the Myc/Max network of TFs (MYC, MAX, and NMYC) have decreased activity in T cells from JIA SF (Figure 2G). These TFs also showed a trend for lower expression in CD4$^+$ T cells from patients' SF compared to healthy-donor-derived CD4$^+$ T cells from PBMCs[20] (Figure S2D). Myc is crucial for Treg function in mice, and loss of Myc in these cells contributes to autoimmune encephalomyelitis driven by uncontrolled CD4$^+$ and CD8$^+$ effector T cell responses.[49]

Overall, these analyses suggest that, while ADs share a general inflammatory and T cell activation program driven by AP-1 and NF-κB, each disease also has its own distinct H3K27ac profile, likely driven by a disease-specific set of TFs.

eGRN reveals TF-driven functional communities in CD4$^+$ T cells

We next studied how differentially active TFs in ADs may contribute to disease mechanisms. We built an eGRN based on paired RNA-seq and H3K27ac ChIP-seq data from PBMC-derived naive CD4$^+$ T cells of 138 healthy donors from the BLUEPRINT consortium,[50] using the eGRN inference tool GRaNIE.[51] Briefly, we used GRaNIE to link TFs to H3K27ac peaks (enhancers) and enhancers to genes. Here, we also kept enhancers that overlapped with AD-associated GWAS variants (Figure 3A; STAR Methods).

The resulting CD4$^+$ T cell eGRN comprises 174 TFs (of which 80 were differentially active in at least one AD) and 4,338 AD-associated GWAS variants connected to 6,980 genes through 7,926 unique enhancers (Figures 3B; Table S3). We validated the network by overlapping T cell-specific expression quantitative trait loci (eQTLs)[52] with enhancer-gene pairs in the eGRN and found them strongly enriched over non-significant pairs (odds ratio [OR] > 5; $p < 1e{-}6$; Figure 3C). Notably, 78% of enhancers in the eGRN are not connected to their nearest gene (Figure 3D), which is in line with previous observations[53] and highlights the capacity of eGRNs to identify distal target genes of an enhancer. The majority (70%) of the genes in the eGRN are linked to enhancers (>2 kb from the TSS), highlighting the importance of considering distal regulatory regions (Figure 3E).

Genes in the eGRN are enriched in GO terms that are highly relevant for T cell biology, including "regulation of T cell receptor signaling," "regulation of NF-κB signaling," and "type I IFN signaling pathway" (Figure 3F, whole eGRN). The eGRN groups into 48 communities when applying Louvain clustering (Table S4), each regulated by a small set of TFs and most enriched for distinct biological processes (Figures 3F and S3). Several communities contain TFs that are differentially active across ADs: community 2, enriched for immunological synapse formation and cellular response to IFN-γ and TNF, is regulated by STAT1 and ETV7 (TFs with the highest degree in this community; Figure S3), which show high activity in SLE (Figure 3D). Community 7, enriched for response to stimulus- and leukocyte-mediated immunity, is mainly regulated by RFX1 and AP-1 complex TFs JUND, FOS, FOSB, and FOSL1, which showed increased activity in all ADs (Figure 2B). Community 5 contains CEBPB, which shows disease-specific activity in Graves' disease (Figure 2E), and community 33 contains MYC, which exhibits disease-specific loss of activity in JIA SF (Figure 2G).

In summary, a naive CD4$^+$ T cell eGRN from healthy donors comprising enhancers, TFs, and genes captures T cell biological processes relevant for ADs, many of which are regulated by TFs that are differentially active in ADs. Thus, this eGRN capturing AD signatures can be used to identify disease-specific TFs, regulatory elements, and their downstream genes.

Disease-specific eGRNs integrating genomic and chromatin data capture potential dysregulated pathways in AD T cells

We next used the CD4$^+$ T cell eGRN to integrate disease-specific genetic (GWAS) and epigenetic (differential TFs and enhancers) evidence to understand T cell dysregulation in ADs. We

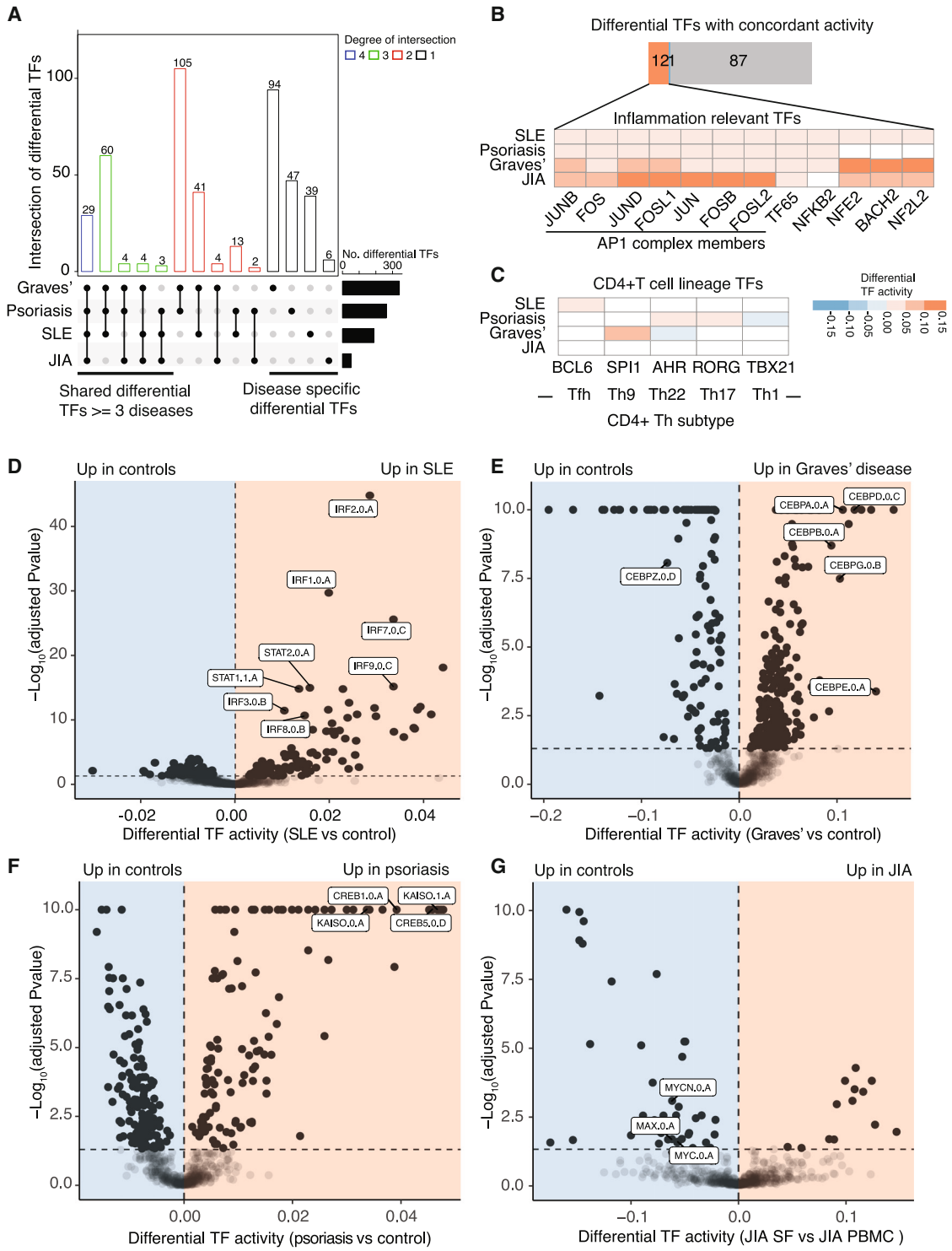

Figure 2. TF activity reveals shared and disease-specific inflammatory T cell processes across ADs

(A) Upset plot of shared and unique significantly differential TFs across diseases.

(B) Inflammation-relevant differential TFs (zoomed in) shared across all ADs.

(C) Disease-specific differential activity of Th-lineage-defining TFs.

(D–G) Volcano plots with differential TF activity versus $\log_{10}$-adjusted *p* value for SLE (D), Graves' disease (E), psoriasis (F), and JIA (G). Selected disease-specific TFs are highlighted. *p* values were quantified with diffTF; see STAR Methods. Number of biological replicates (donors) for each disease is shown in Figure 1A.

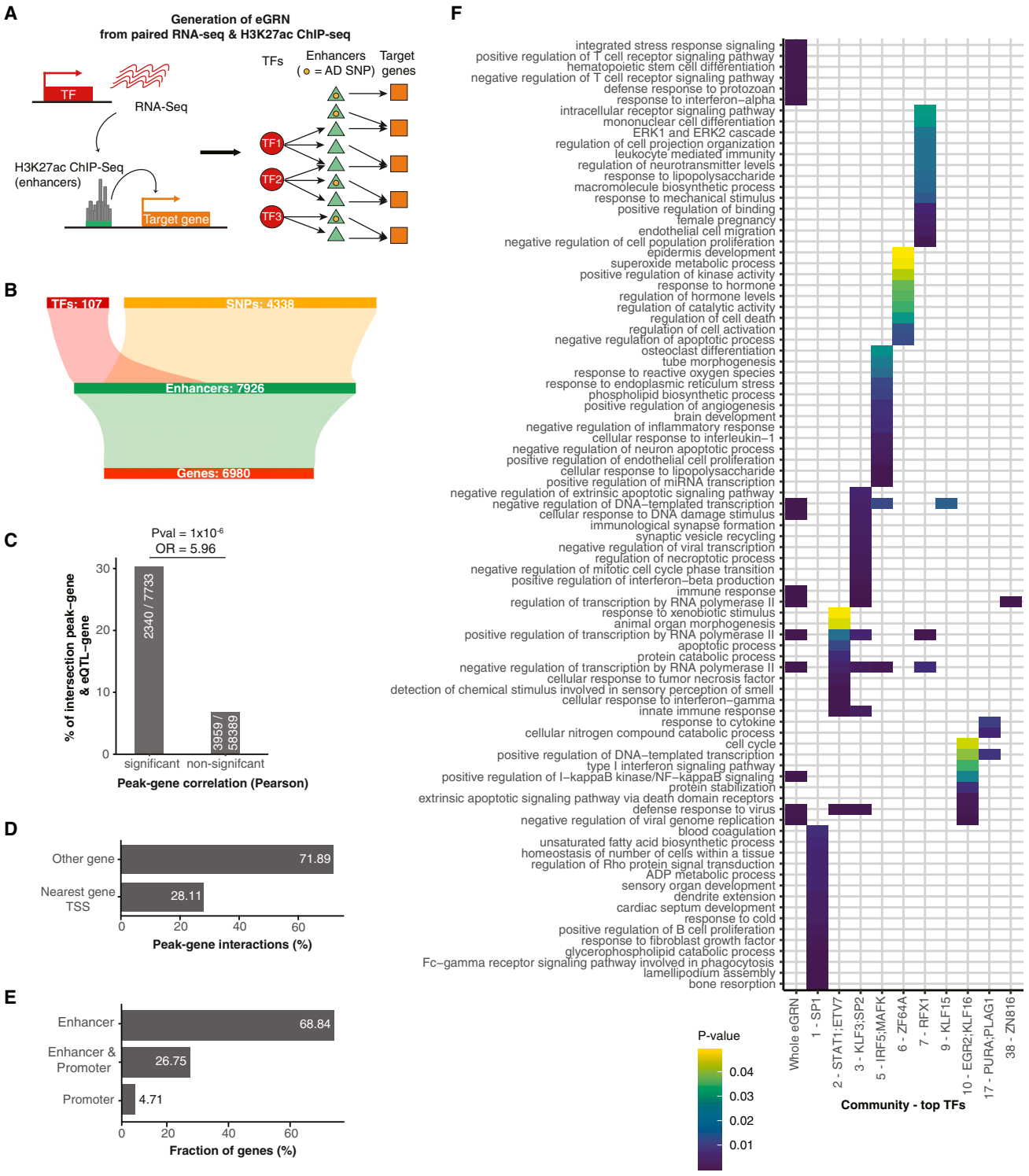

Figure 3. Enhancer-mediated gene regulatory network for CD4⁺ T cells recapitulates known T cell biology

(A) Schematic of T cell eGRN inference from paired RNA and H3K27ac data from healthy naive CD4⁺ T cells.

(B) Schematic representation of eGRN showing total TFs (red), SNPs (yellow), enhancers (green), and genes (orange).

(C) Percentage of overlapping peak-gene connections from eGRN with known eQTL-gene interactions. Data are shown for significant and non-significant peak-gene pairs. Numbers in bars indicate number of overlapping genes/total number of genes. *p* value and odds ratio were calculated using Fisher's exact test.

(legend continued on next page)

annotated the eGRN nodes (TFs and H3K27ac peaks) with four types of molecular disease evidence: (1) TFs with differential activity in ADs versus controls, (2) differential H3K27ac peaks in ADs versus controls, (3) H3K27ac peaks overlapping AD-associated SNPs from the NHGRI-EBI GWAS catalog,[54] and (4) H3K27ac peaks linked to AD GWAS SNPs via a significantly co-localized histone quantitative trait locus.[55] Of these, (1) and (2) reflect epigenetic disease evidence, while (3) and (4) reflect genetic disease evidence.

We split the CD4$^+$ T cell eGRN into four disease-specific eGRNs (for SLE, psoriasis, Graves' disease, and JIA) and one general AD eGRN (schematic in Figure 4A; STAR Methods) This resulted in five different AD eGRNs (Figures 4B; Table S5), with some degree of overlap between two or more networks/diseases, suggesting common disease pathways (Figure 4C).

The genes in the disease-specific AD eGRNs are significantly enriched for genes associated with the respective disease in the OpenTargets platform,[56] while the general AD eGRN was significantly enriched for genes associated with any AD (Figure 4D). Since disease-gene annotations are partially derived from GWASs, which may create a circular argument for the part of our disease eGRNs that is based on genetic evidence, we confirmed a similar enrichment for AD eGRNs without genetic evidence (Figure S4A). Furthermore, the general AD eGRN is enriched for genes that are known drug targets for ADs (Figure 4E).

We next asked whether genetic and epigenetic disease evidence converges onto the same biological pathways. GO term enrichment analysis for genes in the general AD eGRN with only genetic evidence and for those with only epigenetic evidence revealed complementary processes: genes with epigenetic evidence are enriched in immune signaling pathways (i.e., TNF and NOD-like receptor signaling), while genes with genetic evidence are enriched in processes related to T cell differentiation and activation (Figure 4F). Notably, when combining genetic and epigenetic evidence, additional processes like cytokine-mediated signaling and Treg differentiation are enriched. This highlights the power of combining genetic and epigenetic disease evidence in eGRNs for understanding disease mechanisms.

The general AD eGRN captures processes relevant for T cell activation and differentiation, whereas genes in the disease-specific AD eGRNs are enriched in disease-specific pathogenesis processes (Figure 4F). For instance, genes in the SLE network are enriched in type I IFN-related signaling, an important pathway misregulated in SLE.[25,26,42] Moreover, genes linked to TFs in the SLE-specific eGRN were either all up- or all downregulated in patients based on data from Li et al.,[41] further highlighting the disease relevance of these TF-gene connections (Figure S4B). Notably, nearly all target genes of IRF1 and STAT1 (identified as differentially active in SLE patients; Figure 2D) were significantly more highly expressed in SLE patients than in healthy controls (Figures S4C and S4D). Genes in the JIA network were enriched in osteoclast differentiation, a process related to synovial joint inflammation, characterizing JIA patients, as well as regulation of Treg differentiation, a known cell type involved in JIA pathogenesis.[11,20]

Last, we evaluated whether the AD eGRNs were enriched in genes from specific communities from the naive CD4$^+$ T cell eGRN (Figure 3F). Indeed, communities 2 and 7 are enriched across all AD eGRNs, and community 17 is enriched across the general AD, Graves' disease, JIA, and psoriasis eGRNs (Figures 4G and 4H). These communities include TFs that are highly relevant for T cell activation (including AP-1 complex members in community 7, STAT1 in community 2, and PURA in community 17),[30,57] again highlighting shared mechanisms of T cell activation across different ADs. We also identified more specific enrichments of communities across the different AD eGRNs, including community 4 (most enriched in SLE), community 38 (most enriched in psoriasis), and communities 12 and 33 (enriched only in Graves' disease) (Figures 4G and 4H). These results further show that our AD eGRNs recapitulate disease-relevant pathways, with shared and distinct gene signatures.

Identification of Th-subset gene signatures linked to specific AD eGRNs

To further investigate how our eGRNs reflect the activation state of Th cells, we obtained RNA-seq data from five CD4$^+$ T cell subtypes from healthy donors (Th1, Th2, Th17, Treg, and Tfh) that were stimulated with anti-CD3/CD28 beads[58] and defined stimulation-responsive genes as those that are significantly differentially expressed in comparison to resting cells (adjusted $p \leq 0.1$). All AD eGRNs were significantly enriched for stimulation-responsive genes from one or more Th subtypes (Figure 5A; Table S6). The strongest enrichments were observed for Th1, Th17, and Tregs in the psoriasis eGRN and Tregs in the JIA eGRN, in line with the known cell types important in these diseases.[11,20,59] Stimulation-responsive genes in Tregs were also significantly enriched in the Graves' disease and general AD eGRNs (although less strong than in JIA), likely reflecting the crucial role of Tregs in ADs in general.[60]

Next, we asked how enhancer remodeling in AD patients contributes to Th-subset-specific gene expression in response to stimulation. For each disease we focused on the Th subsets that were enriched among the disease-specific eGRNs and correlated the disease-specific changes in H3K27ac signal at enhancers with differential expression upon stimulation of the eGRN-linked genes. We found a positive correlation between expression changes in Tregs with enhancer activation in JIA and SLE and a negative correlation in Graves' disease (Figures 5B and 5C). This may reflect the distinct roles that Tregs play in these diseases and is in line with reports of Treg downregulation in Graves' disease[61] and their upregulation in JIA SF.[11] For JIA, the same positive correlation was observed for enhancers in the JIA-specific eGRN (Figure 5C, bottom right).

For psoriasis, H3K27ac changes were positively correlated with expression changes in stimulated Tregs and negatively

(D) Percentage of peak-gene interactions from the eGRN linked to the transcription start site (TSS) of the nearest gene or another gene.
(E) Percentage of genes from eGRN linked to enhancers, enhancers and promoters, or only promoters.
(F) GO enrichment of biological processes based on all genes included in the eGRN (whole eGRN) and specific communities (indicated by numbers, x axis). Top TFs for each community (based on degree) are highlighted. Colors indicate p values calculated with clusterProfiler (STAR methods).

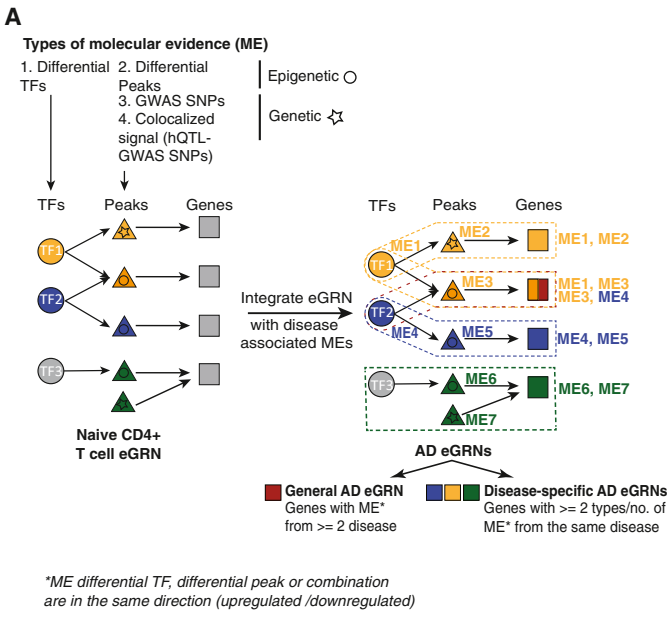

B

eGRN	TFs	Peaks	Genes	Total connections
General AD	29	147	117	468
SLE	37	132	117	264
Psoriasis	39	50	67	161
JIA	22	74	61	196
Graves' disease	92	1112	803	3608

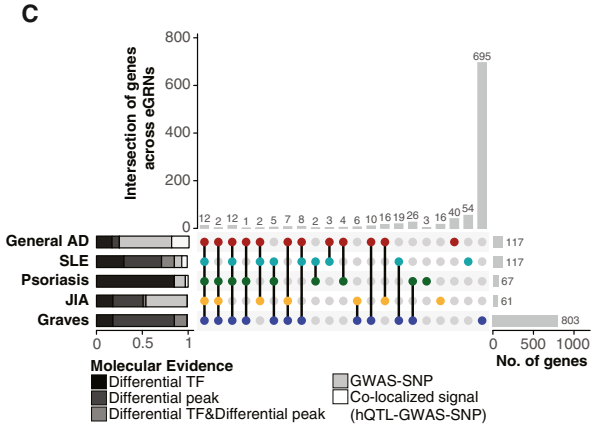

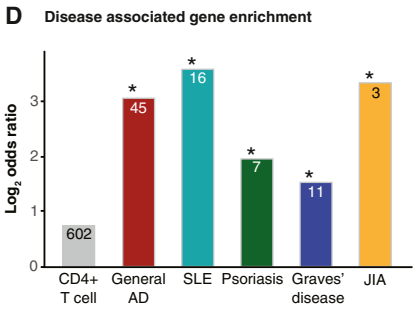

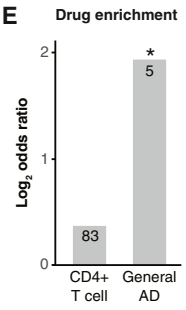

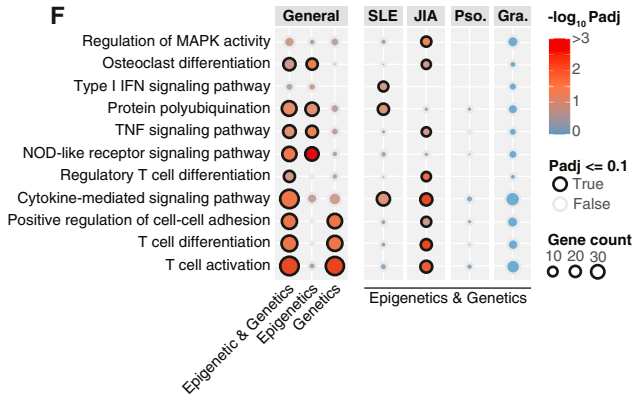

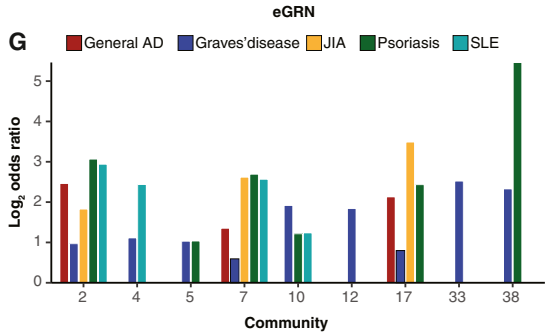

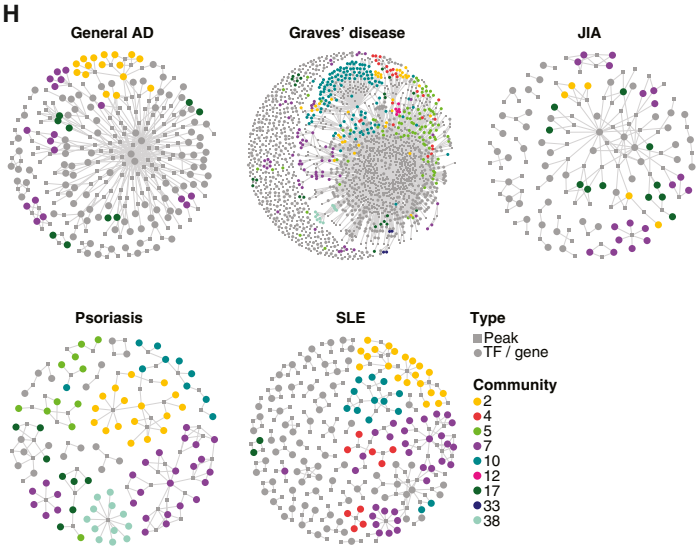

(legend on next page)

correlated with expression changes in stimulated Th17 (Figures 5C and 5D). In line with this, Th17 has been recognized as a crucial T cell subset driving psoriasis pathogenesis, and Tregs in psoriasis can differentiate into IL-17-producing cells that are different from "classical" Th17 cells.[62]

For SLE, we observed a negative correlation of SLE enhancer activity and activation response in Th17 (Figure 5D). Many genes with increased enhancer activity in SLE, and decreased expression in Th17, are related to IFN responses (i.e., IFI44, OAS3, and MX2; Table S6). It has previously been shown that, under inflammatory conditions, Th17 cells produce IFN-γ in addition to IL-17, thereby contributing to autoimmunity.[63] Notably, levels of both IFN-γ and IL-17 are increased in SLE patients,[64] suggesting a potential role for non-classical IFN-γ-producing Th17 cells in the disease pathogenesis.

Overall, we found that disease-specific T cell activation patterns in (non-classical) Th subtypes were reflected in disease-specific enhancer remodeling.

JIA eGRN enhancer-genes within SEs respond to BET inhibitor JQ1, revealing disease-relevant network connections

Super-enhancers (SEs) are stretches or clusters of enhancers with high H3K27ac signal and many TF binding sites.[65] They drive gene expression more than individual enhancers. Moreover, SEs in $CD4^+$ T cells are enriched for AD GWAS SNPs.[17] Here, we used our eGRN framework to investigate the mechanisms underlying this enrichment. We obtained SE annotations for resting and stimulated naive and memory $CD4^+$ T cells[66] and found that enhancers in the JIA, psoriasis, and general AD eGRNs are significantly enriched in T cell-specific SEs (Figure 6A). Furthermore, eGRN enhancers located within SEs showed significantly higher H3K27ac signal in patients versus controls than enhancers not overlapping SEs across all eGRNs except for Graves' disease (Figure 6B). This highlights the relevance of $CD4^+$ T cell-associated SEs in AD-specific H3K27ac remodeling.

To further investigate SEs in the context of eGRNs, we obtained publicly available RNA-seq data from SF-derived $CD4^+$ T cells from JIA patients before and after treatment with the bromodomain and extraterminal (BET) inhibitor JQ1, known to target SEs.[20] We observed that genes connected via the JIA eGRN to SEs that overlapped differential enhancers in JIA were more downregulated upon JQ1 treatment than other genes not connected to SE ($p = 0.1$). JQ1 treatment had no effect on genes in proximity to SE that are not in the JIA eGRN, suggesting JQ1 acts exclusively on SEs that are remodeled in JIA (Figure 6C). Notably, genes in the JIA eGRN were more strongly downregulated than genes linked to SEs by proximity (±2 kb; Figure 6C; $p = 0.008$ if considering unique enhancer-gene pairs and 0.25 if considering unique genes only). The JIA eGRN genes connected to SEs (Figure 6D) include *CTLA4* and *NFAT4*, genes known to be important in T cell activation,[67–69] which show downregulation upon JQ1 treatment.

These observations suggest that the JQ1 treatment (which affects SEs) may act by targeting enhancers and thus affecting their target genes in the JIA eGRN. This provides orthogonal validation of the disease relevance of the enhancer-gene links identified through eGRNs with disease-specific epigenetic and genetic information.

Prioritization and validation of eGRN enhancer-gene pairs potentially important for T cell dysregulation in AD

To identify top genes that are potentially dysregulated across several ADs, we ranked the genes based on the number of AD eGRNs they are part of, the number of molecular disease evidence types, and the total number of molecular evidences. This list was supplemented with information about fine-mapped AD variants, significant expression changes upon T cell stimulation, and known associations with autoimmune conditions (Figure 7A).[56] The top three candidates in our prioritized gene list are *IKZF3*, *CTLA4*, and *CDK12*, which have previously been identified as crucial regulators of T cell activation.[67,70,71]

One enhancer connected to *CTLA4* (chr2:203,930,706–203,942,262) was also connected to *ICOS* and *CD28* in the T cell eGRN (Figure 7B). These three genes, all members of the immunoglobulin super-gene family, play distinct and synergistic roles in the regulation of T cell responses,[68] and their expression is significantly upregulated in all subsets of activated T cells (Figure 7C). Enhancer chr2:203,930,706–203,942,262 (Figure 7B, highlighted in gray) overlaps two differential AD peaks, both downregulated in Graves' disease (Figure 7D), and one upregulated in JIA (Figure 7D). These peaks are connected to the TFs KLF3 and SP2, whose activity was significantly reduced in Graves' disease (Figure 7E).

We validated these enhancer-gene links by CRISPRi in activated primary human T cells using four single-guide RNAs (sgRNAs) targeting enhancer chr2:203,930,706–203,942,262 (sgRNA design in Figure S5A; Table S7). Targeting the enhancer led to a decrease in *ICOS*, *CTLA4*, and *CD28* expression (Figure 7F). The observed downregulation was strongest in *ICOS*, followed by *CTLA4* and *CD28*, in line with their increased genomic distance from the perturbed enhancer (Figure 7B).

Another top prioritized gene was *ANKRD55* (Figure 7A), about which little is described in T cell biology hitherto. *ANKRD55* is identified in all five eGRNs; it is regulated by an enhancer containing four AD-associated genetic variants from multiple sclerosis

Figure 4. AD-specific eGRNs are enriched for disease-associated genes, drug targets, and relevant biological pathways

(A) Overview of AD eGRN generation; ME, molecular evidence.

(B) Numbers of unique TFs, peaks, genes, and total connections in each disease-specific eGRN.

(C) Upset plot showing intersection of genes across disease-specific eGRNs. Bar plot shades indicate proportion of genes with specific ME.

(D and E) Enrichment of disease-specific eGRN genes with disease-associated genes (D) and known drug targets from the Open Targets Platform[56] (E). Numbers indicate gene counts (*Fisher's exact test, $p < 0.05$, and odds ratio > 1).

(F) GO-term enrichment of AD eGRNs. Pso., psoriasis; Gra., Graves' disease. Colors indicate p values calculated with clusterProfiler (STAR methods).

(G) Enrichment of community genes from Figure 3F across AD eGRNs. Only significant enrichments are shown (Fisher's exact test, $p < 0.05$, and odds ratio > 1).

(H) Force-directed visualization of AD eGRNs, with colors representing genes belonging to enriched communities.

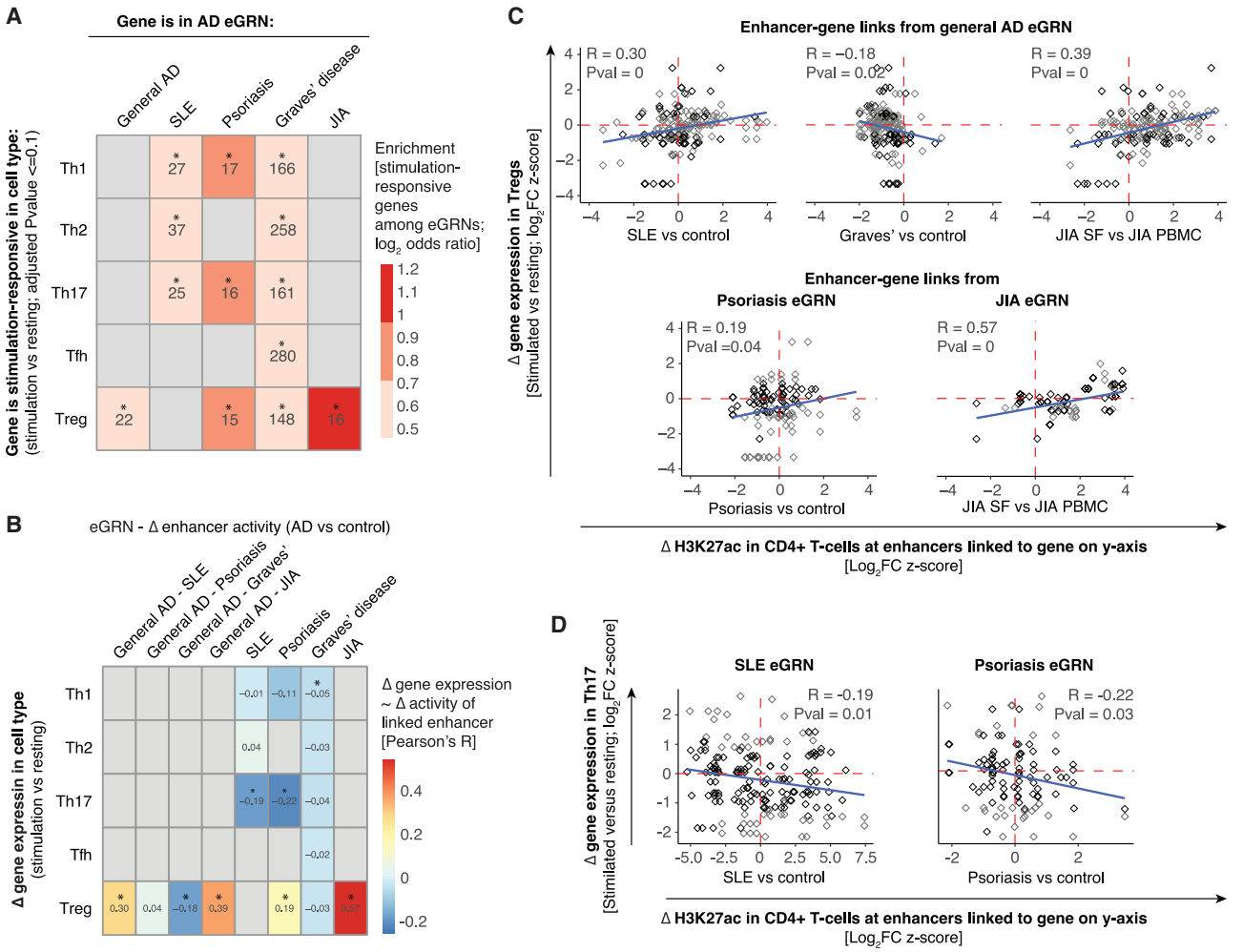

Figure 5. AD-specific eGRNs are enriched in regulatory elements driving gene expression related to Th subset differentiation

(A) Enrichment (log2 odds ratio) of Th subset-specific stimulation-associated genes (rows) within AD eGRNs (columns). Numbers indicate the number of genes per subset (*Fishers' exact test, $p < 0.05$; gray, non-significant).

(B) Correlation (color scale) between expression of Th-subset-specific stimulation-associated genes (rows) and differential peaks from the AD eGRNs (columns). *Pearson correlation, $p < 0.05$.

(C) Pearson correlation of gene expression changes in stimulated versus resting Tregs with H3K27ac changes in CD4$^+$ T cells from AD versus controls. Titles indicate eGRN source for enhancer-gene links. Blue lines, regression. Genes that significantly change expression in Tregs upon stimulation are highlighted in gray (adjusted $p < 0.1$; DESeq2).

(D) Correlation of gene expression changes in stimulated versus resting Th17 with H3K27ac changes in CD4$^+$ T cells from AD versus controls. (C and D) Pearson's R; Pval: p value from Pearson's correlation.

(MS), JIA, rheumatoid arthritis (RA), and inflammatory bowel disease (IBD).[72] In addition, in our eGRN, the enhancer regulating *ANKRD55* (chr5:56,139,147–56,162,711) was also connected to *IL6ST* (Figure 7G), a gene associated with T cell function and disease activity in SLE.[73] The enhancer overlaps two AD-associated peaks downregulated in most ADs we analyzed (Figure 7H).

To confirm the interaction between *ANKRD55* and *IL6ST*, we examined chromatin capture (HiC) data in CD4$^+$ T cells from Bediaga et al.[74] They reported a chromatin loop between the two genes, suggesting direct physical evidence for the enhancer identified in our eGRN (Figure 7I). Notably, Bediaga et al.[74] reported that the interaction between *ANKRD55* and *IL6ST* is significantly stronger in activated versus resting T cells (logFC = 1.01, adjusted p = 5e−05; Figure 7I). In our network, the TF HIC2 is predicted to repress the enhancer at the 5′ end of this loop. Thus, a strengthened interaction between ANKRD55 and IL6ST in activated T cells would bring the repressor HIC2 near the IL6ST promoter, which is in line with the observed decrease in expression of *ANKRD55* and *IL6ST* in activated versus resting CD4$^+$ T cells (Figure 7J). Of note, CRISPRi experiments of this enhancer led to inconsistent results, with IL6ST expression increasing upon CRISPRi (Figures S5B and S5C). This was not due to technical issues, since CRISPRi on the CD4 promoter led to the expected downregulation of the gene (Figure S5D). We rather believe that

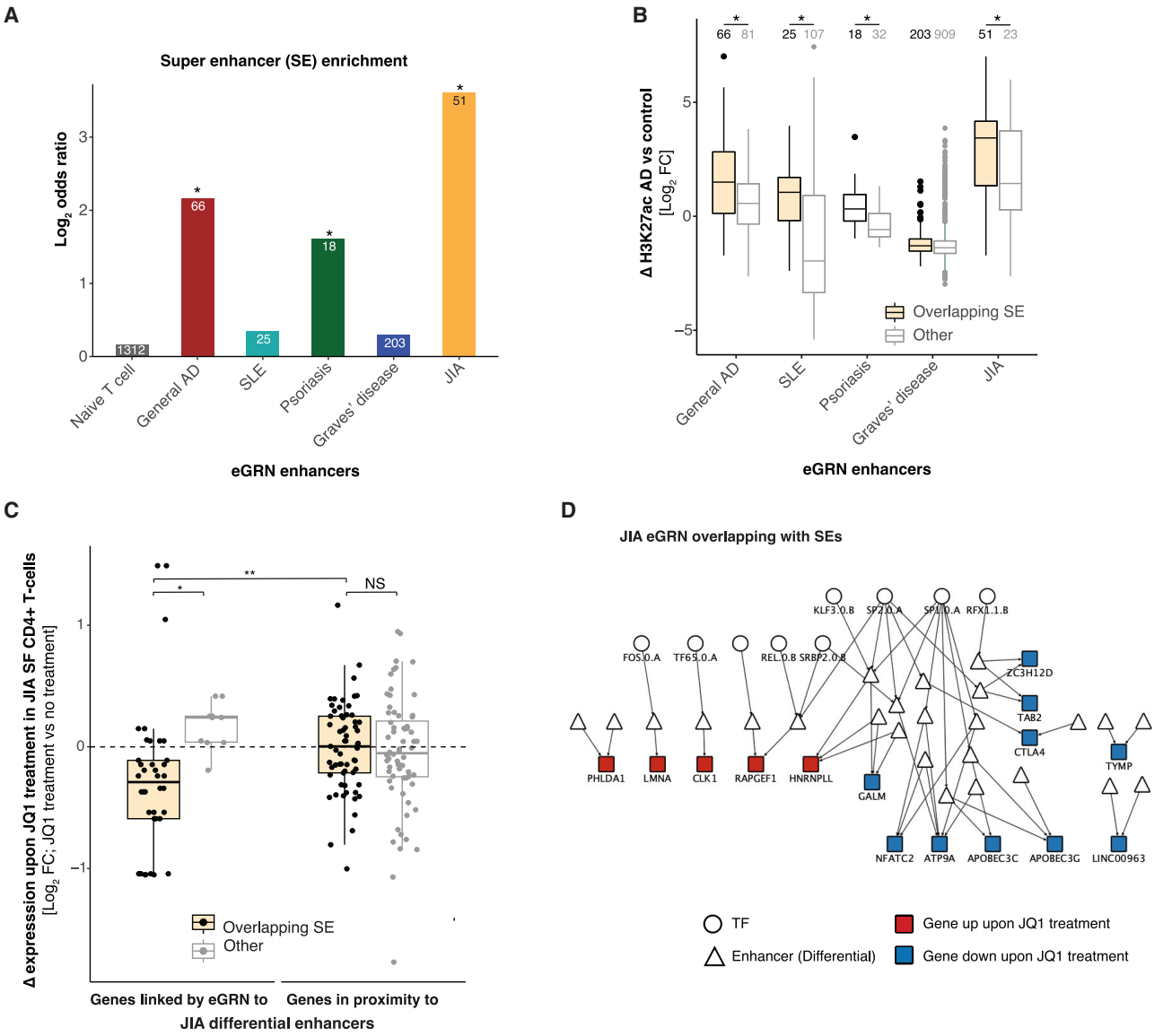

Figure 6. AD eGRNs are significantly enriched in super-enhancers, and genes linked to SEs in the JIA eGRN respond to BET inhibitor treatment

(A) Enrichment (log2 odds ratio) of T cell-specific SEs across naive CD4$^+$ T cell eGRNs and AD-specific eGRNs (*Fisher's exact test, $p < 0.05$). Numbers indicate count of eGRN genes overlapping SEs.

(B) H3K27ac changes in AD versus controls for enhancers from AD-specific eGRNs, categorized into overlap (orange) or no overlap (gray) with T cell-specific SEs. Numbers indicate unique enhancers. *$p < 0.05$ (t test).

(C) Gene expression changes in SF-derived CD4$^+$ T cells from JIA patients treated with BET inhibitor (JQ1$^+$ versus JQ1$^-$) for genes stratified into whether they are linked to JIA-specific differential enhancers via the JIA eGRN or just in proximity of an SE (±2 kb). Based on t test: *$p \leq 0.1$; **$p \leq 0.01$; NS, non-significant).

(D) JIA eGRN with TF, enhancer (overlapping SEs and differential), and gene connection.

the change in chromatin interactions upon T cell activation in this locus (Figure S5E) may interfere with the long-range effects of CRISPRi perturbations (see "Limitations of the study").

These results demonstrate that our eGRNs can be used to identify enhancer-gene links relevant to T cell activation in ADs and can be functionally validated. Similarly, we have generated prioritized lists of genes that are potentially dysregulated in SLE, psoriasis, Graves' disease, and JIA (Table S8). These lists can be used to identify genes and their upstream transcriptional/epigenomic regulators potentially important for T cell function and the pathogenesis of specific ADs.

DISCUSSION

The interpretation of non-coding genetic variants associated with ADs remains a significant challenge. A deeper comprehension of

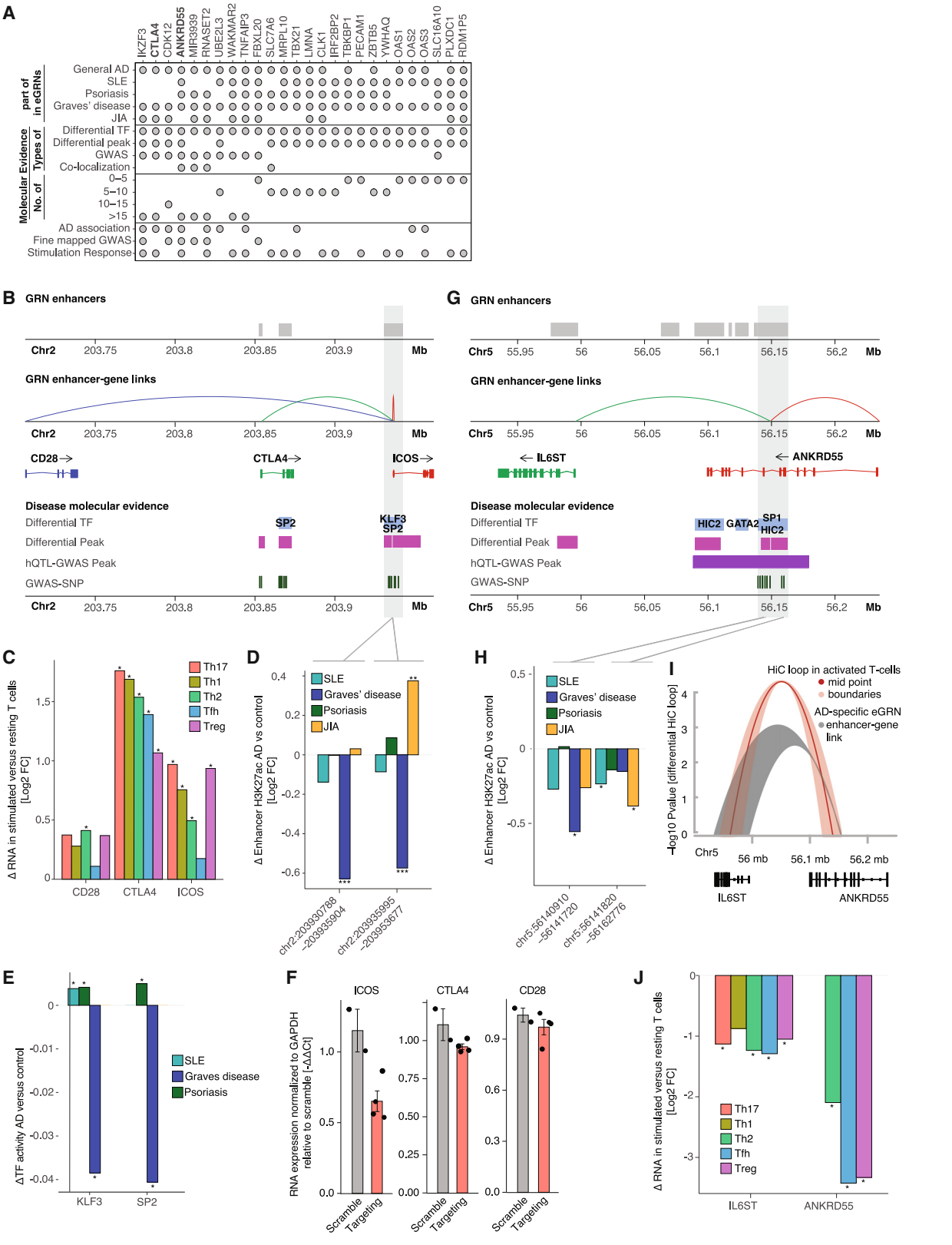

(legend on next page)

the roles of SNPs and regulatory elements in the dysregulation of T cell activation in ADs will improve the understanding of disease mechanisms and identification of new therapeutic targets. To link SNP-harboring enhancers to downstream target genes, we constructed AD-specific eGRNs from CD4$^+$ T cells that can be used to identify targets that inhibit aberrant T cell activation.

We found that AD T cells are characterized by general and disease-specific enhancer signatures and TF activities that potentially regulate disease-relevant pathways. TFs shared across many ADs were related to T cell activation and inflammation, and included members of the AP-1 complex, which are activated through T cell receptor (TCR) and co-stimulatory receptor (i.e., CD28) signaling.[75] This shows that shared dysregulation of T cells in AD is mainly related to T cell activation, likely due to general TCR-antigen binding. Disease-specific TF activity signatures could be driven by signaling related to the nature of the antigen, independent of the TCR. Indeed, in SLE we find an increased activation of IFN-related TFs (in line with increased IFN signaling in these patients[26]), in Graves' disease we find TFs involved in IL-6 signaling[76] (a cytokine increased in the serum of Graves' disease patients[77]), while in psoriasis we find TFs involved in TGF-β signaling[44–46] (implicated in psoriasis pathogenesis[47]).

Integrating eGRNs with expression data from Th cells offers valuable insights into the prevalence and functionality of Th subtypes within the general CD4$^+$ T cell population. In the case of psoriasis, where Th17 cells are considered pivotal drivers of pathogenesis,[10] we found evidence for the presence of Tregs that can differentiate into IL-17-producing cells, distinct from the classical Th17 phenotype[62] and indicative of the dynamic interplay between these cell subsets. Importantly, the histone deacetylase (HDAC) inhibitor trichostatin A is known to inhibit the conversion of Tregs to Th17-like cells.[62] Likewise, in SLE, we found a potential role for non-classical IFN-γ-producing Th17 cells in disease pathogenesis. Over the past years, interest in the therapeutic inhibition of Th17 cells in ADs has grown. However, these cells display high levels of plasticity, and their origin and exact pathogenic function in autoimmunity are poorly understood. Classical approaches to inhibit Th17 cells in autoimmunity, including IL-17A blockade, may not be effective against "non-classical" Th17 subtypes,[78] demonstrating the need for a better understanding of the exact disease-associated Th subtypes. Our findings not only emphasize the heterogeneity of T cell responses in AD but also shed light on potential therapeutic targets, for example, through the modulation of specific enhancers linked to genes driving specific Th subsets.

We also show that AD-specific eGRNs are enriched in SEs that regulate processes related to T cell activation and inflammation. BET and Mediator proteins are crucial for the activity of SEs,[79] and their inhibition is pursued as a therapeutic strategy to control the aberrant transcription of genes in cancer and other diseases.[80] JQ1 is a well-studied BET inhibitor, which represses the expression of T cell-activation-related genes in memory/effector T cells in JIA.[20] In line with this, we show that JQ1 selectively inhibits the expression of genes linked to SEs identified in our JIA-specific eGRN. Since we also found an enrichment of SEs in our general AD and psoriasis eGRNs, these results can potentially be extrapolated to other ADs. Indeed, JQ1 treatment was shown to alleviate general inflammation and decrease the number of CD4$^+$IL-17A$^+$ T cells in imiquimod-induced psoriasis mouse models,[81,82] further highlighting the therapeutic potential of BET inhibitors in the treatment of ADs.

Enhancers are traditionally linked to their nearest genes using proximity-based methods, even though they can regulate their target genes over large genomic distances,[83] and autoimmune-associated SNPs in non-coding regions often affect distal genes.[84] Our eGRNs can identify distal enhancer-target gene links that would be missed using conventional proximity-based methods. As an example, we identified a distal enhancer linked to *CTLA4* (distance of 60,052 bp) that was also linked to *ICOS* (TSS, 0 bp) and *CD28* (222,190 bp). This enhancer overlaps six SNPs (rs56324422, rs4675374, rs11571305, rs11571306, rs4335928, and rs10932031) that are associated with celiac disease.[54,85] Although these SNPs have mainly been associated with *ICOS* expression (the most proximal gene), we show that perturbation of the enhancer harboring these SNPs also affects the more distal *CTLA4* and *CD28*, which also play crucial roles in regulating T cell responses and immune tolerance.[68] Other examples we studied are *IL6ST* and *ANKRD55*, which we found linked to an enhancer that overlaps a T cell-specific SE and harbors many AD-associated SNPs. One of these SNPs, rs6859219, is associated with increased *ANKRD55* levels in CD4$^+$ T cells.[86] Moreover, increased *IL6ST* expression is associated with Th17 differentiation (a cell type highly relevant in ADs) in mice.[87] We identified HIC2 as a repressor of *ANKRD55* and *IL6ST* expression, in line with its described repressor function.[88] SNPs in the

Figure 7. Prioritization and validation of disease-relevant enhancers from AD eGRNs

(A) Ranked list of prioritized AD-relevant genes based on their presence in AD-specific eGRNs and associated molecular evidence.

(B) Genomic context of *ICOS*/*CTLA4*/*CD28*, showing links to AD eGRN enhancers (top gray boxes), differential TF binding sites (blue boxes, TFs highlighted in black), differential H3K27ac peaks (pink boxes), hQTL-GWAS peaks (purple boxes), and AD-associated GWAS-SNPs (dark green stripes).

(C) Differential expression of *ICOS*, *CTLA4*, and *CD28* in stimulated versus resting CD4$^+$ T cells is shown as log2 fold change.

(D) Differential H3K27ac signal for enhancers linked to *ICOS*/*CTLA4*/*CD28* in AD patients versus controls is shown as log2 fold change.

(E) Differential activity of KLF3 and SP2 in AD patients versus controls is shown.

(F) Expression of *ICOS*/*CTLA4*/*CD28* following CRISPRi-mediated enhancer perturbation in CD4$^+$ T cells, shown as mRNA expression relative to a non-targeting control gRNA for the targeting (Targeting) and non-targeting controls (Scramble), mean ± SEM.

(G) Genomic context of *ANKRD55*/*IL6ST* and their links to AD eGRN enhancers.

(H) Log2 fold change in H3K27ac signal of enhancers linked to *ANKRD55*/*IL6ST* in AD patients.

(I) Loop based on chromatin capture (HiC) data obtained from Bediaga et al.[74] shown at 25 kb resolution (red line; shading indicates resolution) and eGRN loop between *ANKRD55* intron and *IL6ST*.

(J) Log2 fold change in *IL6ST* and *ANKRD55* gene expression in stimulated versus resting CD4$^+$ T cells (x axis). For all: $^*p \leq 0.05$, $^{**}p \leq 0.01$, $^{***}p \leq 0.001$, calculated using t test.

associated enhancer potentially disrupt the repressive function of HIC2, thereby leading to increased *ANKRD55* and *IL6ST* expression. HIC2 function has not been studied in T cells or other immune cells hitherto, but our analysis points to it as a potentially important regulator in the context of ADs. This demonstrates the potential of eGRNs to link AD-associated enhancers harboring SNPs to downstream genes and upstream regulators, to uncover regulatory mechanisms driving T cell dysfunction in autoimmunity. Since the generation of disease-specific eGRNs is based on the mapping of disease-specific evidence (including GWAS SNPs) onto a naive $CD4^+$ T cell eGRN, future risk loci from GWASs can be integrated to further refine the existing eGRNs.

Taking our results altogether, we demonstrate that eGRNs are powerful tools to study disease-specific dysregulation of T cells. They can be used to pinpoint alterations in the regulatory landscapes that contribute to the development of ADs and provide a basis for developing new therapeutic approaches.

Limitations of the study

- CRISPRi-based validations of enhancer-gene interactions: we attempted functional validation of the interaction between *ANKRD55* and *IL6ST* by CRISPRi targeting their associated enhancer, which coincided with the 5′ end of the chromatin loop between these two genes. This experiment showed upregulation of *IL6ST*, which was contradictory to the general repressive effect of CRISPRi (Figure S5C). Inspection of the 3D landscape around the locus region revealed complex interactions with many up- and downregulated loops during T cell activation (Figure S5E). This highlights the challenge of using CRISPRi for validating distal enhancer-gene interactions in complex loci, where the CRISPRi guides may interfere with loop formation, leading to unexpected outcomes.
- Future work should address the unexpected upregulation of the *IL6ST* locus upon CRISPRi targeting of the enhancer. Based on our data and analyses, one hypothesis to be tested is whether the CRISPR machinery interferes with the complex 3D genome rearrangement during T cell activation and thus prevents the repressive TF HIC2 from interacting with *IL6ST.* This could be tested using alternative CRISPR approaches that do not rely on the machinery being present during the activation (e.g., CRISPR-Cas9) or by measuring the dynamics of the chromatin interactions during the CRISPRi perturbation.
- Patient samples: it is important to note that, in the context of JIA, our observations of the changes in the epigenomic landscape and differential TF activity are based on SF-specific signatures rather than comparisons between healthy controls and JIA patients. The ideal control samples would have been $CD4^+$ T cells from SF of healthy children. However, since there is no diagnostic procedure in which SF is taken from joints of healthy children, this is ethically not possible. Moreover, in healthy knee joints, SF typically contains very low numbers of T cells. The accepted view in the field is that for JIA, the tissue-resident cells are actively associated with disease, while the T cells in PBMCs are not active.[11,20,89–98] Thus, our approach is in line with the best practice in the field.

RESOURCE AVAILABILITY

Lead contact

Requests for further information and resources and reagents should be directed to and will be fulfilled by the lead contact, Judith Zaugg (judith.zaugg@embl.de).

Materials availability

This study did not generate new unique reagents.

Data and code availability

De-identified patient H3K27ac data are deposited at the NCBI GEO (GSE251736) and are publicly available as of the date of publication. In addition, this paper analyzes existing data, of which accession numbers are listed in the key resources table. All original code has been deposited at https://gitfront.io/r/user-2800625/inXS3mECwiLE/AD-Enhancer-Remodelling/ and is publicly available as of the date of publication. Any additional information is available from the lead contact upon request.

ACKNOWLEDGMENTS

We thank Annique Claringbould, for feedback and discussions on integration of GWAS data, and the staff at the EMBL Genomics and Flow Cytometry Core Facility, for sample preparation and data generation. We thank the Hanke Gwendolin Bauersachs for critical reading of the manuscript and the Zaugg group for scientific discussions. We are grateful to all individuals who donated the samples included in this study. The graphical abstract and Figure 1A were created with BioRender. N.D., N.H.S., and J.B.Z. acknowledge funding from GSK through the EMBL-GSK collaboration framework (3000032294). N.H.S. and J.B.Z. acknowledge funding from the EMBL Infection Biology Transversal theme. K.Kisand. and P.P. acknowledge funding from the Estonian Research Council (PRG377 and PRG1117) and from the Centre of Excellence for Genomics and Translational Medicine funded by the European Regional Development Fund (Project no. 2014-2020.4.01.15-0012). A.R.-P. has been the recipient of a postdoctoral fellowship granted by Fundación Ramón Areces (2017-T2/BMD-5532). This project is co-funded by the European Union (ERC, EpiNicheAML, 101044873) to J.B.Z. Views and opinions expressed are, however, those of the authors only and do not necessarily reflect those of the European Union or the European Research Council. Neither the European Union nor the granting authority can be held responsible for them.

AUTHOR CONTRIBUTIONS

Conceptualization, N.D. and J.B.Z.; methodology, N.D., C.A., and A.R.-P.; software, N.D., N.H.S., C.A., and A.R.-P.; validation, N.D., N.H.S., and D.M.; formal analysis, N.D. and N.H.S.; investigation, D.M., K.Kisand., and E.K.; resources, K.Kisand., K.Kingo., R.K., K.U., L.S., P.P., and J.B.Z.; data curation, N.D. and N.H.S.; writing – original draft, N.D., N.H.S., and J.B.Z.; writing – review & editing, N.D., N.H.S., K.Kisand., D.M., C.A., A.R.P., L.S., P.P., N.N., and J.B.Z.; visualization, N.D. and N.H.S.; supervision, N.N. and J.B.Z.; funding acquisition, N.N. and J.B.Z.

DECLARATION OF INTERESTS

The authors declare no conflict of interest.

STAR★METHODS

Detailed methods are provided in the online version of this paper and include the following:

- KEY RESOURCES TABLE
- EXPERIMENTAL MODEL AND STUDY PARTICIPANT DETAILS
- METHOD DETAILS

SUPPLEMENTAL INFORMATION

Supplemental information can be found online at https://doi.org/10.1016/j.celrep.2024.114810.

Received: December 23, 2023
Revised: July 16, 2024
Accepted: September 16, 2024
Published: October 9, 2024

REFERENCES

1. Saravia, J., Chapman, N.M., and Chi, H. (2019). Helper T cell differentiation. Cell. Mol. Immunol. *16*, 634–643. https://doi.org/10.1038/s41423-019-0220-6.
2. Zhu, X., and Zhu, J. (2020). CD4 T helper cell subsets and related human immunological disorders. Int. J. Mol. Sci. *21*, 8011. https://doi.org/10.3390/ijms21218011.
3. Veldhoen, M., Uyttenhove, C., van Snick, J., Helmby, H., Westendorf, A., Buer, J., Martin, B., Wilhelm, C., and Stockinger, B. (2008). Transforming growth factor-beta "reprograms" the differentiation of T helper 2 cells and promotes an interleukin 9-producing subset. Nat. Immunol. *9*, 1341–1346. https://doi.org/10.1038/ni.1659.
4. Eyerich, S., Eyerich, K., Pennino, D., Carbone, T., Nasorri, F., Pallotta, S., Cianfarani, F., Odorisio, T., Traidl-Hoffmann, C., Behrendt, H., et al. (2009). Th22 cells represent a distinct human T cell subset involved in epidermal immunity and remodeling. J. Clin. Invest. *119*, 3573–3585. https://doi.org/10.1172/JCI40202.
5. Abdirama, D., Tesch, S., Grießbach, A.-S., von Spee-Mayer, C., Humrich, J.Y., Stervbo, U., Babel, N., Meisel, C., Alexander, T., Biesen, R., et al. (2021). Nuclear antigen-reactive CD4+ T cells expand in active systemic lupus erythematosus, produce effector cytokines, and invade the kidneys. Kidney Int. *99*, 238–246. https://doi.org/10.1016/j.kint.2020.05.051.
6. Arakawa, A., Siewert, K., Stöhr, J., Besgen, P., Kim, S.-M., Rühl, G., Nickel, J., Vollmer, S., Thomas, P., Krebs, S., et al. (2015). Melanocyte antigen triggers autoimmunity in human psoriasis. J. Exp. Med. *212*, 2203–2212. https://doi.org/10.1084/jem.20151093.
7. Kamphuis, S., Hrafnkelsdóttir, K., Klein, M.R., de Jager, W., Haverkamp, M.H., van Bilsen, J.H.M., Albani, S., Kuis, W., Wauben, M.H.M., and Prakken, B.J. (2006). Novel self-epitopes derived from aggrecan, fibrillin, and matrix metalloproteinase-3 drive distinct autoreactive T-cell responses in juvenile idiopathic arthritis and in health. Arthritis Res. Ther. *8*, R178. https://doi.org/10.1186/ar2088.
8. Dayan, C.M., Londei, M., Corcoran, A.E., Grubeck-Loebenstein, B., James, R.F., Rapoport, B., and Feldmann, M. (1991). Autoantigen recognition by thyroid-infiltrating T cells in Graves disease. Proc. Natl. Acad. Sci. USA *88*, 7415–7419. https://doi.org/10.1073/pnas.88.16.7415.
9. Blanco, P., Ueno, H., and Schmitt, N. (2016). T follicular helper (Tfh) cells in lupus: Activation and involvement in SLE pathogenesis. Eur. J. Immunol. *46*, 281–290. https://doi.org/10.1002/eji.201545760.
10. Li, B., Huang, L., Lv, P., Li, X., Liu, G., Chen, Y., Wang, Z., Qian, X., Shen, Y., Li, Y., and Fang, W. (2020). The role of Th17 cells in psoriasis. Immunol. Res. *68*, 296–309. https://doi.org/10.1007/s12026-020-09149-1.
11. Mijnheer, G., Servaas, N.H., Leong, J.Y., Boltjes, A., Spierings, E., Chen, P., Lai, L., Petrelli, A., Vastert, S., de Boer, R.J., et al. (2023). Compartmentalization and persistence of dominant (regulatory) T cell clones indicates antigen skewing in juvenile idiopathic arthritis. Elife *12*, e79016. https://doi.org/10.7554/eLife.79016.
12. Copland, A., and Bending, D. (2018). Foxp3 molecular dynamics in treg in juvenile idiopathic arthritis. Front. Immunol. *9*, 2273. https://doi.org/10.3389/fimmu.2018.02273.
13. Kocjan, T., Wraber, B., Repnik, U., and Hojker, S. (2000). Changes in Th1/Th2 cytokine balance in Graves' disease. Pflügers Archiv *440*, R94–R95.
14. Bluestone, J.A., Bour-Jordan, H., Cheng, M., and Anderson, M. (2015). T cells in the control of organ-specific autoimmunity. J. Clin. Invest. *125*, 2250–2260. https://doi.org/10.1172/JCI78089.
15. Gough, S.C.L., and Simmonds, M.J. (2007). The HLA Region and Autoimmune Disease: Associations and Mechanisms of Action. Curr. Genom. *8*, 453–465. https://doi.org/10.2174/138920207783591690.
16. Wellcome Trust Case Control Consortium (2007). Genome-wide association study of 14,000 cases of seven common diseases and 3,000 shared controls. Nature *447*, 661–678. https://doi.org/10.1038/nature05911.
17. Farh, K.K.-H., Marson, A., Zhu, J., Kleinewietfeld, M., Housley, W.J., Beik, S., Shoresh, N., Whitton, H., Ryan, R.J.H., Shishkin, A.A., et al. (2015). Genetic and epigenetic fine mapping of causal autoimmune disease variants. Nature *518*, 337–343. https://doi.org/10.1038/nature13835.
18. Wang, Z., Chang, C., and Lu, Q. (2017). Epigenetics of CD4+ T cells in autoimmune diseases. Curr. Opin. Rheumatol. *29*, 361–368. https://doi.org/10.1097/BOR.0000000000000393.
19. Limbach, M., Saare, M., Tserel, L., Kisand, K., Eglit, T., Sauer, S., Axelsson, T., Syvänen, A.-C., Metspalu, A., Milani, L., and Peterson, P. (2016). Epigenetic profiling in CD4+ and CD8+ T cells from Graves' disease patients reveals changes in genes associated with T cell receptor signaling. J. Autoimmun. *67*, 46–56. https://doi.org/10.1016/j.jaut.2015.09.006.
20. Peeters, J.G.C., Vervoort, S.J., Tan, S.C., Mijnheer, G., de Roock, S., Vastert, S.J., Nieuwenhuis, E.E.S., van Wijk, F., Prakken, B.J., Creyghton, M.P., et al. (2015). Inhibition of Super-Enhancer Activity in Autoinflammatory Site-Derived T Cells Reduces Disease-Associated Gene Expression. Cell Rep. *12*, 1986–1996. https://doi.org/10.1016/j.celrep.2015.08.046.
21. Gu, Z., and Hübschmann, D. (2023). rGREAT: an R/bioconductor package for functional enrichment on genomic regions. Bioinformatics *39*, btac745. https://doi.org/10.1093/bioinformatics/btac745.
22. Pawlak, M., Ho, A.W., and Kuchroo, V.K. (2020). Cytokines and transcription factors in the differentiation of CD4+ T helper cell subsets and induction of tissue inflammation and autoimmunity. Curr. Opin. Immunol. *67*, 57–67. https://doi.org/10.1016/j.coi.2020.09.001.
23. Sakaguchi, S., Ono, M., Setoguchi, R., Yagi, H., Hori, S., Fehervari, Z., Shimizu, J., Takahashi, T., and Nomura, T. (2006). Foxp3+ CD25+ CD4+ natural regulatory T cells in dominant self-tolerance and autoimmune disease. Immunol. Rev. *212*, 8–27. https://doi.org/10.1111/j.0105-2896.2006.00427.x.
24. Moreau, J.M., Gouirand, V., and Rosenblum, M.D. (2021). T-Cell Adhesion in Healthy and Inflamed Skin. JID Innov. *1*, 100014. https://doi.org/10.1016/j.xjidi.2021.100014.

25. Pan, Q., Liu, Z., Liao, S., Ye, L., Lu, X., Chen, X., Li, Z., Li, X., Xu, Y.-Z., and Liu, H. (2019). Current mechanistic insights into the role of infection in systemic lupus erythematosus. Biomed. Pharmacother. *117*, 109122. https://doi.org/10.1016/j.biopha.2019.109122.

26. Ríos-Garcés, R., and Cervera, R. (2020). Targeting interferon I in SLE: a promising new perspective. Lancet. Rheumatol. *2*, e581–e582. https://doi.org/10.1016/S2665-9913(20)30288-5.

27. Berest, I., Arnold, C., Reyes-Palomares, A., Palla, G., Rasmussen, K.D., Giles, H., Bruch, P.-M., Huber, W., Dietrich, S., Helin, K., and Zaugg, J.B. (2019). Quantification of Differential Transcription Factor Activity and Multiomics-Based Classification into Activators and Repressors: diffTF. Cell Rep. *29*, 3147–3159.e12. https://doi.org/10.1016/j.celrep.2019.10.106.

28. Liu, T., Zhang, L., Joo, D., and Sun, S.-C. (2017). NF-κB signaling in inflammation. Signal Transduct. Targeted Ther. *2*, 17023. https://doi.org/10.1038/sigtrans.2017.23.

29. Renoux, F., Stellato, M., Haftmann, C., Vogetseder, A., Huang, R., Subramaniam, A., Becker, M.O., Blyszczuk, P., Becher, B., Distler, J.H.W., et al. (2020). The AP1 transcription factor fosl2 promotes systemic autoimmunity and inflammation by repressing treg development. Cell Rep. *31*, 107826. https://doi.org/10.1016/j.celrep.2020.107826.

30. Yukawa, M., Jagannathan, S., Vallabh, S., Kartashov, A.V., Chen, X., Weirauch, M.T., and Barski, A. (2020). AP-1 activity induced by co-stimulation is required for chromatin opening during T cell activation. J. Exp. Med. *217*, e20182009. https://doi.org/10.1084/jem.20182009.

31. Ruan, Q., Kameswaran, V., Zhang, Y., Zheng, S., Sun, J., Wang, J., DeVirgiliis, J., Liou, H.-C., Beg, A.A., and Chen, Y.H. (2011). The Th17 immune response is controlled by the Rel-RORγ-RORγ T transcriptional axis. J. Exp. Med. *208*, 2321–2333. https://doi.org/10.1084/jem.20110462.

32. Trifari, S., Kaplan, C.D., Tran, E.H., Crellin, N.K., and Spits, H. (2009). Identification of a human helper T cell population that has abundant production of interleukin 22 and is distinct from T(H)-17, T(H)1 and T(H)2 cells. Nat. Immunol. *10*, 864–871. https://doi.org/10.1038/ni.1770.

33. Szabo, S.J., Kim, S.T., Costa, G.L., Zhang, X., Fathman, C.G., and Glimcher, L.H. (2000). A novel transcription factor, T-bet, directs Th1 lineage commitment. Cell *100*, 655–669. https://doi.org/10.1016/s0092-8674(00)80702-3.

34. Palmer, M.T., and Weaver, C.T. (2010). Autoimmunity: increasing suspects in the CD4+ T cell lineup. Nat. Immunol. *11*, 36–40. https://doi.org/10.1038/ni.1802.

35. Choi, J., Diao, H., Faliti, C.E., Truong, J., Rossi, M., Bélanger, S., Yu, B., Goldrath, A.W., Pipkin, M.E., and Crotty, S. (2020). Bcl-6 is the nexus transcription factor of T follicular helper cells via repressor-of-repressor circuits. Nat. Immunol. *21*, 777–789. https://doi.org/10.1038/s41590-020-0706-5.

36. Gerlach, K., Hwang, Y., Nikolaev, A., Atreya, R., Dornhoff, H., Steiner, S., Lehr, H.-A., Wirtz, S., Vieth, M., Waisman, A., et al. (2014). TH9 cells that express the transcription factor PU.1 drive T cell-mediated colitis via IL-9 receptor signaling in intestinal epithelial cells. Nat. Immunol. *15*, 676–686. https://doi.org/10.1038/ni.2920.

37. Kagami, S., Rizzo, H.L., Lee, J.J., Koguchi, Y., and Blauvelt, A. (2010). Circulating Th17, Th22, and Th1 cells are increased in psoriasis. J. Invest. Dermatol. *130*, 1373–1383. https://doi.org/10.1038/jid.2009.399.

38. Benham, H., Norris, P., Goodall, J., Wechalekar, M.D., FitzGerald, O., Szentpetery, A., Smith, M., Thomas, R., and Gaston, H. (2013). Th17 and Th22 cells in psoriatic arthritis and psoriasis. Arthritis Res. Ther. *15*, R136. https://doi.org/10.1186/ar4317.

39. Kim, S.J., Lee, K., and Diamond, B. (2018). Follicular helper T cells in systemic lupus erythematosus. Front. Immunol. *9*, 1793. https://doi.org/10.3389/fimmu.2018.01793.

40. Ren, X., and Chen, H. (2022). Changes in Th9 and Th17 lymphocytes and functional cytokines and their relationship with thyroid-stimulating hormone receptor antibodies at different stages of graves' disease. Front. Immunol. *13*, 919681. https://doi.org/10.3389/fimmu.2022.919681.

41. Li, Z., Wang, Z., Sun, T., Liu, S., Ding, S., and Sun, L. (2022). Identifying key genes in CD4+ T cells of systemic lupus erythematosus by integrated bioinformatics analysis. Front. Genet. *13*, 941221. https://doi.org/10.3389/fgene.2022.941221.

42. Lopez-Dominguez, R., Toro-Dominguez, D., Martorell-Marugan, J., Garcia-Moreno, A., Holland, C.H., Saez-Rodriguez, J., Goldman, D., Petri, M.A., Alarcon-Riquelme, M.E., and Carmona-Saez, P. (2021). Transcription factor activity inference in systemic lupus erythematosus. Life *11*, 299. https://doi.org/10.3390/life11040299.

43. Poli, V. (1998). The role of C/EBP isoforms in the control of inflammatory and native immunity functions. J. Biol. Chem. *273*, 29279–29282. https://doi.org/10.1074/jbc.273.45.29279.

44. Bassey-Archibong, B.I., Kwiecien, J.M., Milosavljevic, S.B., Hallett, R.M., Rayner, L.G.A., Erb, M.J., Crawford-Brown, C.J., Stephenson, K.B., Bédard, P.A., Hassell, J.A., and Daniel, J.M. (2016). Kaiso depletion attenuates transforming growth factor-β signaling and metastatic activity of triple-negative breast cancer cells. Oncogenesis *5*, e208. https://doi.org/10.1038/oncsis.2016.17.

45. Liu, G., Ding, W., Neiman, J., and Mulder, K.M. (2006). Requirement of Smad3 and CREB-1 in mediating transforming growth factor-beta (TGF beta) induction of TGF beta 3 secretion. J. Biol. Chem. *281*, 29479–29490. https://doi.org/10.1074/jbc.M600579200.

46. Feng, J., Han, X., Yuan, Y., Cho, C.K., Janečková, E., Guo, T., Pareek, S., Rahman, M.S., Zheng, B., Bi, J., et al. (2022). TGF-β signaling and Creb5 cooperatively regulate Fgf18 to control pharyngeal muscle development. Elife *11*, e80405. https://doi.org/10.7554/eLife.80405.

47. Han, G., Williams, C.A., Salter, K., Garl, P.J., Li, A.G., and Wang, X.-J. (2010). A role for TGFbeta signaling in the pathogenesis of psoriasis. J. Invest. Dermatol. *130*, 371–377. https://doi.org/10.1038/jid.2009.252.

48. Liu, Y., Wang, H., Cook, C., Taylor, M.A., North, J.P., Hailer, A., Shou, Y., Sadik, A., Kim, E., Purdom, E., et al. (2022). Defining Patient-Level Molecular Heterogeneity in Psoriasis Vulgaris Based on Single-Cell Transcriptomics. Front. Immunol. *13*, 842651. https://doi.org/10.3389/fimmu.2022.842651.

49. Saravia, J., Zeng, H., Dhungana, Y., Bastardo Blanco, D., Nguyen, T.-L.M., Chapman, N.M., Wang, Y., Kanneganti, A., Liu, S., Raynor, J.L., et al. (2020). Homeostasis and transitional activation of regulatory T cells require c-Myc. Sci. Adv. *6*, eaaw6443. https://doi.org/10.1126/sciadv.aaw6443.

50. Bujold, D., Morais, D.A.d.L., Gauthier, C., Côté, C., Caron, M., Kwan, T., Chen, K.C., Laperle, J., Markovits, A.N., Pastinen, T., et al. (2016). The international human epigenome consortium data portal. Cell Syst. *3*, 496–499.e2. https://doi.org/10.1016/j.cels.2016.10.019.

51. Kamal, A., Arnold, C., Claringbould, A., Moussa, R., Servaas, N.H., Kholmatov, M., Daga, N., Nogina, D., Mueller-Dott, S., Reyes-Palomares, A., et al. (2021). GRaNIE and GRaNPA: Inference and evaluation of enhancer-mediated gene regulatory networks applied to study macrophages. Preprint at bioRxiv. https://doi.org/10.1101/2021.12.18.473290.

52. Schmiedel, B.J., Singh, D., Madrigal, A., Valdovino-Gonzalez, A.G., White, B.M., Zapardiel-Gonzalo, J., Ha, B., Altay, G., Greenbaum, J.A., McVicker, G., et al. (2018). Impact of genetic polymorphisms on human immune cell gene expression. Cell *175*, 1701–1715.e16. https://doi.org/10.1016/j.cell.2018.10.022.

53. Reyes-Palomares, A., Gu, M., Grubert, F., Berest, I., Sa, S., Kasowski, M., Arnold, C., Shuai, M., Srivas, R., Miao, S., et al. (2020). Remodeling of active endothelial enhancers is associated with aberrant gene-regulatory networks in pulmonary arterial hypertension. Nat. Commun. *11*, 1673. https://doi.org/10.1038/s41467-020-15463-x.

54. Buniello, A., MacArthur, J.A.L., Cerezo, M., Harris, L.W., Hayhurst, J., Malangone, C., McMahon, A., Morales, J., Mountjoy, E., Sollis, E.,

et al. (2019). The NHGRI-EBI GWAS Catalog of published genome-wide association studies, targeted arrays and summary statistics 2019. Nucleic Acids Res. *47*, D1005–D1012. https://doi.org/10.1093/nar/gky1120.

55. Chen, L., Ge, B., Casale, F.P., Vasquez, L., Kwan, T., Garrido-Martín, D., Watt, S., Yan, Y., Kundu, K., Ecker, S., et al. (2016). Genetic drivers of epigenetic and transcriptional variation in human immune cells. Cell *167*, 1398–1414.e24. https://doi.org/10.1016/j.cell.2016.10.026.
56. Carvalho-Silva, D., Pierleoni, A., Pignatelli, M., Ong, C., Fumis, L., Karamanis, N., Carmona, M., Faulconbridge, A., Hercules, A., McAuley, E., et al. (2019). Open Targets Platform: new developments and updates two years on. Nucleic Acids Res. *47*, D1056–D1065. https://doi.org/10.1093/nar/gky1133.
57. Afkarian, M., Sedy, J.R., Yang, J., Jacobson, N.G., Cereb, N., Yang, S.Y., Murphy, T.L., and Murphy, K.M. (2002). T-bet is a STAT1-induced regulator of IL-12R expression in naïve CD4+ T cells. Nat. Immunol. *3*, 549–557. https://doi.org/10.1038/ni794.
58. Calderon, D., Nguyen, M.L.T., Mezger, A., Kathiria, A., Müller, F., Nguyen, V., Lescano, N., Wu, B., Trombetta, J., Ribado, J.V., et al. (2019). Landscape of stimulation-responsive chromatin across diverse human immune cells. Nat. Genet. *51*, 1494–1505. https://doi.org/10.1038/s41588-019-0505-9.
59. Lowes, M.A., Kikuchi, T., Fuentes-Duculan, J., Cardinale, I., Zaba, L.C., Haider, A.S., Bowman, E.P., and Krueger, J.G. (2008). Psoriasis vulgaris lesions contain discrete populations of Th1 and Th17 T cells. J. Invest. Dermatol. *128*, 1207–1211. https://doi.org/10.1038/sj.jid.5701213.
60. Dominguez-Villar, M., and Hafler, D.A. (2018). Regulatory T cells in autoimmune disease. Nat. Immunol. *19*, 665–673. https://doi.org/10.1038/s41590-018-0120-4.
61. Chen, Z., Liu, Y., Hu, S., Zhang, M., Shi, B., and Wang, Y. (2021). Decreased Treg Cell and TCR Expansion Are Involved in Long-Lasting Graves' Disease. Front. Endocrinol. *12*, 632492. https://doi.org/10.3389/fendo.2021.632492.
62. Bovenschen, H.J., van de Kerkhof, P.C., van Erp, P.E., Woestenenk, R., Joosten, I., and Koenen, H.J.P.M. (2011). Foxp3+ regulatory T cells of psoriasis patients easily differentiate into IL-17A-producing cells and are found in lesional skin. J. Invest. Dermatol. *131*, 1853–1860. https://doi.org/10.1038/jid.2011.139.
63. Hirota, K., Duarte, J.H., Veldhoen, M., Hornsby, E., Li, Y., Cua, D.J., Ahlfors, H., Wilhelm, C., Tolaini, M., Menzel, U., et al. (2011). Fate mapping of IL-17-producing T cells in inflammatory responses. Nat. Immunol. *12*, 255–263. https://doi.org/10.1038/ni.1993.
64. Yazici, M.U., Orhan, D., Kale, G., Besbas, N., and Ozen, S. (2014). Studying IFN-gamma, IL-17 and FOXP3 in pediatric lupus nephritis. Pediatr. Nephrol. *29*, 853–862. https://doi.org/10.1007/s00467-013-2695-1.
65. Pott, S., and Lieb, J.D. (2015). What are super-enhancers? Nat. Genet. *47*, 8–12. https://doi.org/10.1038/ng.3167.
66. Hnisz, D., Abraham, B.J., Lee, T.I., Lau, A., Saint-André, V., Sigova, A.A., Hoke, H.A., and Young, R.A. (2013). Super-enhancers in the control of cell identity and disease. Cell *155*, 934–947. https://doi.org/10.1016/j.cell.2013.09.053.
67. Ueda, H., Howson, J.M.M., Esposito, L., Heward, J., Snook, H., Chamberlain, G., Rainbow, D.B., Hunter, K.M.D., Smith, A.N., Di Genova, G., et al. (2003). Association of the T-cell regulatory gene CTLA4 with susceptibility to autoimmune disease. Nature *423*, 506–511. https://doi.org/10.1038/nature01621.
68. Rudd, C.E., and Schneider, H. (2003). Unifying concepts in CD28, ICOS and CTLA4 co-receptor signalling. Nat. Rev. Immunol. *3*, 544–556. https://doi.org/10.1038/nri1131.
69. Lee, J.-U., Kim, L.-K., and Choi, J.-M. (2018). Revisiting the concept of targeting NFAT to control T cell immunity and autoimmune diseases. Front. Immunol. *9*, 2747. https://doi.org/10.3389/fimmu.2018.02747.
70. Zou, Y., Liu, B., Li, L., Yin, Q., Tang, J., Jing, Z., Huang, X., Zhu, X., and Chi, T. (2022). IKZF3 deficiency potentiates chimeric antigen receptor T cells targeting solid tumors. Cancer Lett. *524*, 121–130. https://doi.org/10.1016/j.canlet.2021.10.016.
71. Li, Y., Zhang, H., Li, Q., Zou, P., Huang, X., Wu, C., and Tan, L. (2020). CDK12/13 inhibition induces immunogenic cell death and enhances anti-PD-1 anticancer activity in breast cancer. Cancer Lett. *495*, 12–21. https://doi.org/10.1016/j.canlet.2020.09.011.
72. Ugidos, N., Mena, J., Baquero, S., Alloza, I., Azkargorta, M., Elortza, F., and Vandenbroeck, K. (2019). Interactome of the autoimmune risk protein ANKRD55. Front. Immunol. *10*, 2067. https://doi.org/10.3389/fimmu.2019.02067.
73. Mohd Shukri, N.D., Farah Izati, A., Wan Ghazali, W.S., Che Hussin, C.M., and Wong, K.K. (2021). Cd3+cd4+gp130+ T cells are associated with worse disease activity in systemic lupus erythematosus patients. Front. Immunol. *12*, 675250. https://doi.org/10.3389/fimmu.2021.675250.
74. Bediaga, N.G., Coughlan, H.D., Johanson, T.M., Garnham, A.L., Naselli, G., Schröder, J., Fearnley, L.G., Bandala-Sanchez, E., Allan, R.S., Smyth, G.K., and Harrison, L.C. (2021). Multi-level remodelling of chromatin underlying activation of human T cells. Sci. Rep. *11*, 528. https://doi.org/10.1038/s41598-020-80165-9.
75. Rincón, M., and Flavell, R.A. (1994). AP-1 transcriptional activity requires both T-cell receptor-mediated and co-stimulatory signals in primary T lymphocytes. EMBO J. *13*, 4370–4381. https://doi.org/10.1002/j.1460-2075.1994.tb06757.x.
76. Alonzi, T., Gorgoni, B., Screpanti, I., Gulino, A., and Poli, V. (1997). Interleukin-6 and CAAT/enhancer binding protein beta-deficient mice act as tools to dissect the IL-6 signalling pathway and IL-6 regulation. Immunobiology *198*, 144–156. https://doi.org/10.1016/s0171-2985(97)80035-6.
77. Salvi, M., Girasole, G., Pedrazzoni, M., Passeri, M., Giuliani, N., Minelli, R., Braverman, L.E., and Roti, E. (1996). Increased serum concentrations of interleukin-6 (IL-6) and soluble IL-6 receptor in patients with Graves' disease. J. Clin. Endocrinol. Metab. *81*, 2976–2979. https://doi.org/10.1210/jcem.81.8.8768861.
78. Basdeo, S.A., Cluxton, D., Sulaimani, J., Moran, B., Canavan, M., Orr, C., Veale, D.J., Fearon, U., and Fletcher, J.M. (2017). Ex-Th17 (Nonclassical Th1) Cells Are Functionally Distinct from Classical Th1 and Th17 Cells and Are Not Constrained by Regulatory T Cells. J. Immunol. *198*, 2249–2259. https://doi.org/10.4049/jimmunol.1600737.
79. Crump, N.T., Ballabio, E., Godfrey, L., Thorne, R., Repapi, E., Kerry, J., Tapia, M., Hua, P., Lagerholm, C., Filippakopoulos, P., et al. (2021). BET inhibition disrupts transcription but retains enhancer-promoter contact. Nat. Commun. *12*, 223. https://doi.org/10.1038/s41467-020-20400-z.
80. Claringbould, A., and Zaugg, J.B. (2021). Enhancers in disease: molecular basis and emerging treatment strategies. Trends Mol. Med. *27*, 1060–1073. https://doi.org/10.1016/j.molmed.2021.07.012.
81. Nadeem, A., Al-Harbi, N.O., Al-Harbi, M.M., El-Sherbeeny, A.M., Ahmad, S.F., Siddiqui, N., Ansari, M.A., Zoheir, K.M.A., Attia, S.M., Al-Hosaini, K.A., and Al-Sharary, S.D. (2015). Imiquimod-induced psoriasis-like skin inflammation is suppressed by BET bromodomain inhibitor in mice through RORC/IL-17A pathway modulation. Pharmacol. Res. *99*, 248–257. https://doi.org/10.1016/j.phrs.2015.06.001.
82. Sun, X., and Yang, P. (2021). Inhibition of BRD4 inhibits proliferation and promotes apoptosis of psoriatic keratinocytes. Biomed. Eng. Online *20*, 107. https://doi.org/10.1186/s12938-021-00943-y.
83. Bondarenko, V.A., Liu, Y.V., Jiang, Y.I., and Studitsky, V.M. (2003). Communication over a large distance: enhancers and insulators. Biochem. Cell. Biol. *81*, 241–251. https://doi.org/10.1139/o03-051.
84. Chen, X.-F., Guo, M.-R., Duan, Y.-Y., Jiang, F., Wu, H., Dong, S.-S., Zhou, X.-R., Thynn, H.N., Liu, C.-C., Zhang, L., et al. (2020). Multiomics dissection of molecular regulatory mechanisms underlying autoimmune-associated

noncoding SNPs. JCI Insight *5*, e136477. https://doi.org/10.1172/jci.insight.136477.

85. Trynka, G., Hunt, K.A., Bockett, N.A., Romanos, J., Mistry, V., Szperl, A., Bakker, S.F., Bardella, M.T., Bhaw-Rosun, L., Castillejo, G., et al. (2011). Dense genotyping identifies and localizes multiple common and rare variant association signals in celiac disease. Nat. Genet. *43*, 1193–1201. https://doi.org/10.1038/ng.998.

86. Lopez de Lapuente, A., Feliú, A., Ugidos, N., Mecha, M., Mena, J., Astobiza, I., Riera, J., Carrillo-Salinas, F.J., Comabella, M., Montalban, X., et al. (2016). Novel Insights into the Multiple Sclerosis Risk Gene ANKRD55. J. Immunol. *196*, 4553–4565. https://doi.org/10.4049/jimmunol.1501205.

87. Liao, W., Lin, J.-X., Wang, L., Li, P., and Leonard, W.J. (2011). Modulation of cytokine receptors by IL-2 broadly regulates differentiation into helper T cell lineages. Nat. Immunol. *12*, 551–559. https://doi.org/10.1038/ni.2030.

88. Deltour, S., Pinte, S., Guérardel, C., and Leprince, D. (2001). Characterization of HRG22, a human homologue of the putative tumor suppressor gene HIC1. Biochem. Biophys. Res. Commun. *287*, 427–434. https://doi.org/10.1006/bbrc.2001.5624.

89. Grose, R.H., Millard, D.J., Mavrangelos, C., Barry, S.C., Zola, H., Nicholson, I.C., Cham, W.T., Boros, C.A., and Krumbiegel, D. (2012). Comparison of blood and synovial fluid th17 and novel peptidase inhibitor 16 Treg cell subsets in juvenile idiopathic arthritis. J. Rheumatol. *39*, 2021–2031. https://doi.org/10.3899/jrheum.111421.

90. Wienke, J., de Roock, S., Swart, J., Martens, A., Wulffraat, N., and Prakken, B. (2014). Mesenchymal stromal cells suppress synovial fluid-derived t cells from juvenile idiopathic arthritis patients in vitro. Pediatr. Rheumatol. *12*, P129. https://doi.org/10.1186/1546-0096-12-S1-P129.

91. Ruprecht, C.R., Gattorno, M., Ferlito, F., Gregorio, A., Martini, A., Lanzavecchia, A., and Sallusto, F. (2005). Coexpression of CD25 and CD27 identifies FoxP3+ regulatory T cells in inflamed synovia. J. Exp. Med. *201*, 1793–1803. https://doi.org/10.1084/jem.20050085.

92. Mijnheer, G., Lutter, L., Mokry, M., van der Wal, M., Scholman, R., Fleskens, V., Pandit, A., Tao, W., Wekking, M., Vervoort, S., et al. (2021). Conserved human effector Treg cell transcriptomic and epigenetic signature in arthritic joint inflammation. Nat. Commun. *12*, 2710. https://doi.org/10.1038/s41467-021-22975-7.

93. Bending, D., Pesenacker, A.M., Ursu, S., Wu, Q., Lom, H., Thirugnanabalan, B., and Wedderburn, L.R. (2014). Hypomethylation at the regulatory T cell-specific demethylated region in CD25hi T cells is decoupled from FOXP3 expression at the inflamed site in childhood arthritis. J. Immunol. *193*, 2699–2708. https://doi.org/10.4049/jimmunol.1400599.

94. Moncrieffe, H., Nistala, K., Kamhieh, Y., Evans, J., Eddaoudi, A., Eaton, S., and Wedderburn, L.R. (2010). High expression of the ectonucleotidase CD39 on T cells from the inflamed site identifies two distinct populations, one regulatory and one memory T cell population. J. Immunol. *185*, 134–143. https://doi.org/10.4049/jimmunol.0803474.

95. de Kleer, I.M., Wedderburn, L.R., Taams, L.S., Patel, A., Varsani, H., Klein, M., de Jager, W., Pugayung, G., Giannoni, F., Rijkers, G., et al. (2004). CD4+CD25bright regulatory T cells actively regulate inflammation in the joints of patients with the remitting form of juvenile idiopathic arthritis. J. Immunol. *172*, 6435–6443. https://doi.org/10.4049/jimmunol.172.10.6435.

96. Ferguson, I.D., Griffin, P., Michel, J.J., Yano, H., Gaffen, S.L., Mueller, R.G., Dvergsten, J.A., Piganelli, J.D., Rosenkranz, M.E., Kietz, D.A., and Vallejo, A.N. (2018). T Cell Receptor-Independent, CD31/IL-17A-Driven Inflammatory Axis Shapes Synovitis in Juvenile Idiopathic Arthritis. Front. Immunol. *9*, 1802. https://doi.org/10.3389/fimmu.2018.01802.

97. Nistala, K., Adams, S., Cambrook, H., Ursu, S., Olivito, B., de Jager, W., Evans, J.G., Cimaz, R., Bajaj-Elliott, M., and Wedderburn, L.R. (2010). Th17 plasticity in human autoimmune arthritis is driven by the inflammatory environment. Proc. Natl. Acad. Sci. USA *107*, 14751–14756. https://doi.org/10.1073/pnas.1003852107.

98. Olivito, B., Simonini, G., Ciullini, S., Moriondo, M., Betti, L., Gambineri, E., Cantarini, L., De Martino, M., Azzari, C., and Cimaz, R. (2009). Th17 transcription factor RORC2 is inversely correlated with FOXP3 expression in the joints of children with juvenile idiopathic arthritis. J. Rheumatol. *36*, 2017–2024. https://doi.org/10.3899/jrheum.090066.

99. Taylor, K.E., Ansel, K.M., Marson, A., Criswell, L.A., and Farh, K.K.-H. (2021). PICS2: next-generation fine mapping via probabilistic identification of causal SNPs. Bioinformatics *37*, 3004–3007. https://doi.org/10.1093/bioinformatics/btab122.

100. Kulakovskiy, I.V., Vorontsov, I.E., Yevshin, I.S., Sharipov, R.N., Fedorova, A.D., Rumynskiy, E.I., Medvedeva, Y.A., Magana-Mora, A., Bajic, V.B., Papatsenko, D.A., et al. (2018). HOCOMOCO: towards a complete collection of transcription factor binding models for human and mouse via large-scale ChIP-Seq analysis. Nucleic Acids Res. *46*, D252–D259. https://doi.org/10.1093/nar/gkx1106.

101. Bolger, A.M., Lohse, M., and Usadel, B. (2014). Trimmomatic: A flexible trimmer for Illumina sequence data. Bioinformatics *30*, 2114–2120. https://doi.org/10.1093/bioinformatics/btu170.

102. Langmead, B., and Salzberg, S.L. (2012). Fast gapped-read alignment with Bowtie 2. Nat. Methods *9*, 357–359. https://doi.org/10.1038/nmeth.1923.

103. Danecek, P., Bonfield, J.K., Liddle, J., Marshall, J., Ohan, V., Pollard, M.O., Whitwham, A., Keane, T., McCarthy, S.A., Davies, R.M., and Li, H. (2021). Twelve years of SAMtools and BCFtools. GigaScience *10*, giab008. https://doi.org/10.1093/gigascience/giab008.

104. Gaspar, J.M. (2018). Improved peak-calling with MACS2. Preprint at bioRxiv. https://doi.org/10.1101/496521.

105. Dobin, A., Davis, C.A., Schlesinger, F., Drenkow, J., Zaleski, C., Jha, S., Batut, P., Chaisson, M., and Gingeras, T.R. (2013). STAR: ultrafast universal RNA-seq aligner. Bioinformatics *29*, 15–21. https://doi.org/10.1093/bioinformatics/bts635.

106. Lawrence, M., Huber, W., Pagès, H., Aboyoun, P., Carlson, M., Gentleman, R., Morgan, M.T., and Carey, V.J. (2013). Software for computing and annotating genomic ranges. PLoS Comput. Biol. *9*, e1003118. https://doi.org/10.1371/journal.pcbi.1003118.

107. Love, M.I., Huber, W., and Anders, S. (2014). Moderated estimation of fold change and dispersion for RNA-seq data with DESeq2. Genome Biol. *15*, 550. https://doi.org/10.1186/s13059-014-0550-8.

108. Yu, G., Wang, L.-G., Han, Y., and He, Q.-Y. (2012). clusterProfiler: an R package for comparing biological themes among gene clusters. OMICS *16*, 284–287. https://doi.org/10.1089/omi.2011.0118.

109. Ambrosini, G., Groux, R., and Bucher, P. (2018). PWMScan: a fast tool for scanning entire genomes with a position-specific weight matrix. Bioinformatics *34*, 2483–2484. https://doi.org/10.1093/bioinformatics/bty127.

110. Giambartolomei, C., Vukcevic, D., Schadt, E.E., Franke, L., Hingorani, A.D., Wallace, C., and Plagnol, V. (2014). Bayesian test for colocalisation between pairs of genetic association studies using summary statistics. PLoS Genet. *10*, e1004383. https://doi.org/10.1371/journal.pgen.1004383.

111. Chen, S., Sanjana, N.E., Zheng, K., Shalem, O., Lee, K., Shi, X., Scott, D.A., Song, J., Pan, J.Q., Weissleder, R., et al. (2015). Genome-wide CRISPR screen in a mouse model of tumor growth and metastasis. Cell *160*, 1246–1260. https://doi.org/10.1016/j.cell.2015.02.038.

112. Schraivogel, D., Gschwind, A.R., Milbank, J.H., Leonce, D.R., Jakob, P., Mathur, L., Korbel, J.O., Merten, C.A., Velten, L., and Steinmetz, L.M. (2020). Targeted Perturb-seq enables genome-scale genetic screens in single cells. Nat. Methods *17*, 629–635. https://doi.org/10.1038/s41592-020-0837-5.

113. Tsoi, L.C., Spain, S.L., Knight, J., Ellinghaus, E., Stuart, P.E., Capon, F., Ding, J., Li, Y., Tejasvi, T., Gudjonsson, J.E., et al. (2012). Identification of

15 new psoriasis susceptibility loci highlights the role of innate immunity. Nat. Genet. *44*, 1341–1348. https://doi.org/10.1038/ng.2467.

114. Bentham, J., Morris, D.L., Graham, D.S.C., Pinder, C.L., Tombleson, P., Behrens, T.W., Martín, J., Fairfax, B.P., Knight, J.C., Chen, L., et al. (2015). Genetic association analyses implicate aberrant regulation of innate and adaptive immunity genes in the pathogenesis of systemic lupus erythematosus. Nat. Genet. *47*, 1457–1464. https://doi.org/10.1038/ng.3434.

115. de Lange, K.M., Moutsianas, L., Lee, J.C., Lamb, C.A., Luo, Y., Kennedy, N.A., Jostins, L., Rice, D.L., Gutierrez-Achury, J., Ji, S.-G., et al. (2017). Genome-wide association study implicates immune activation of multiple integrin genes in inflammatory bowel disease. Nat. Genet. *49*, 256–261. https://doi.org/10.1038/ng.3760.

116. Okada, Y., Wu, D., Trynka, G., Raj, T., Terao, C., Ikari, K., Kochi, Y., Ohmura, K., Suzuki, A., Yoshida, S., et al. (2014). Genetics of rheumatoid arthritis contributes to biology and drug discovery. Nature *506*, 376–381. https://doi.org/10.1038/nature12873.

117. Demenais, F., Margaritte-Jeannin, P., Barnes, K.C., Cookson, W.O.C., Altmüller, J., Ang, W., Barr, R.G., Beaty, T.H., Becker, A.B., Beilby, J., et al. (2018). Multiancestry association study identifies new asthma risk loci that colocalize with immune-cell enhancer marks. Nat. Genet. *50*, 42–53. https://doi.org/10.1038/s41588-017-0014-7.

STAR★METHODS

KEY RESOURCES TABLE

REAGENT or RESOURCE	SOURCE	IDENTIFIER
Antibodies		
Anti-human H3K27ac	Abcam	ab4729; RRID: AB_2118291
Biological samples		
SLE, psoriasis and matched healthy donor peripheral blood samples	University of Tartu (Estonia)	https://ut.ee/en
$CD4^+$ T cells from healthy donors for CRISPRi experiments	AllCells	Naive CD4+/CD45RA+ Helper T cell
LentiX HEK293T cells	Takara	632180
Chemicals, peptides, and recombinant proteins		
Ficoll Paque Plus	GE Healthcare	GE17-1440-02
CD4 MicroBeads, human	Miltenyi	130-045-101
Dynabeads™ M-280 Sheep Anti-Mouse IgG	Invitrogen	11202D
Dynabeads™ M-280 Sheep Anti-Rabbit IgG	Invitrogen	11203D
RNase Cocktail™ Enzyme Mix	Ambion	AM2286
Proteinase K	Thermo Scientific	EO0492
DMEM medium	Gibco	41965-039
FBS Supreme	PanBiotech	P30-3031
GlutaMAX™ Supplement	Gibco	35050061
Sodium pyruvate (NaPyr)	Gibco	11360070
Non-Essential Amino Acid (NEAA)	Gibco	11140050
Penicillin–Streptomycin	Gibco	15070063
Opti-MEM	Gibco	31985070
Lipofectamine™ 3000	Invitrogen	L3000015
Viralboost reagent	Alstem	VB100
Lenti-X concentrator	Takara	631232
RPMI-1640	Gibco	52400025
2-Mercaptoethanol	Gibco	31350010
Recombinant Human IL-2	Peprotech	200-02
CD3/CD28 Dynabeads™	Gibco	11161
Puromycin	Gibco	A111380
DRAQ7™ Dye	Biostatus	DR77524
SuperScript IV Reverse Transcriptase	Invitrogen	18090010
SYBR-Green PCR master mix	Applied Biosystems	4309155
Critical commercial assays		
MinElute PCR Purification Kit	Qiagen	28004
Plasmid DNA Mini-Prep Kit	Qiagen	12123
RNeasy mini kit	Qiagen	74004
Qubit™ RNA Broad Range assay kit	Thermo Scientific	Q10211
NEBNext Ultra II DNA Library Prep Kit	New England Biolabs	E7645L
Deposited data		
Raw and analyzed data	This paper	GEO: GSE251736
Human reference genome NCBI build 38, GRCh38	Genome Reference Consortium	http://www.ncbi.nlm.nih.gov/projects/genome/assembly/grc/human/

(*Continued on next page*)

Continued

REAGENT or RESOURCE	SOURCE	IDENTIFIER
GENCODE Human release 28, GRCh38.p12	The GENCODE Project	https://www.gencodegenes.org/human/release_28.html
PICS 2.0 Autoimmune Disease and GWAS catalog SNPs	Taylor et al.[99]	https://pics2.ucsf.edu
HOCOMOCO v11 TF binding models	Kulakovskliy et al.[100]	https://hocomoco11.autosome.org
RNA- and H3K27ac ChIP-seq data from CD4$^+$ T cells from SF and PBMCs of JIA patients all diagnosed with oligoarticular JIA with active disease at the time of sampling. Patients underwent therapeutic joint aspiration and PB was drawn at the same time.	Peeters et al.[20]	GEO: GSE71595 & GEO: GSE71596
H3K27ac ChIP-seq data from CD4$^+$ T cells from Graves' disease patients and matched healthy donors	Limbach et al.[19]	GEO: GSE71957
H3K27ac ChIP-seq data and RNA-seq data from CD4$^+$ T cells from 138 healthy donors.	Blueprint consortium	EGA: EGAD00001002673 & EGA: EGAD00001002671
ATAC-seq and RNA-seq data from stimulated CD4$^+$ T helper subsets.	Calderon et al.[58]	GEO: GSE118189 & GEO: GSE118165
RNA-seq data from CD4$^+$ T cells from SLE and healthy controls.	Li et al.[41]	GEO: GSE97263
scRNA-seq data of CD45$^+$ cells derived from skin biopsies of psoriasis and healthy controls.	Liu et al.[48]	https://zenodo.org/records/6529821#.Ynh_aoxBwuW
Hi-C-seq of resting and activated CD4$^+$ T cells.	Bediaga et al.[74]	GEO: GSE126117
Software and algorithms		
FASTQC	Babraham Bioinformatics	https://www.bioinformatics.babraham.ac.uk/projects/fastqc/
Trimmomatic	Bolger et al.[101]	http://www.usadellab.org/cms/?page=trimmomatic
Bowtie2	Langmead et al.[102]	https://bowtie-bio.sourceforge.net/bowtie2/index.shtml
SAMtools	Danecek et al.[103]	http://www.htslib.org/
Picard	Broad institute	https://broadinstitute.github.io/picard/
MACS2	Gaspar et al.[104]	https://pypi.org/project/MACS2/
DiffBind	Rory Stark	https://bioconductor.org/packages/release/bioc/html/DiffBind.html
STAR	Dobin et al.[105]	https://github.com/alexdobin/STAR
GenomicAlignments	Lawrence et al.[106]	https://bioconductor.org/packages/release/bioc/html/GenomicAlignments.html
DESeq2	Love et al.[107]	https://bioconductor.org/packages/release/bioc/html/DESeq2.html
diffTF	Berest & Arnold et al.[27]	https://git.embl.de/grp-zaugg/diffTF
GRaNIE	Kamal & Arnold et al.[51]	https://grp-zaugg.embl-community.io/GRaNIE/
clusterProfiler	Yu et al.[108]	https://bioconductor.org/packages/release/bioc/html/clusterProfiler.html
rGREAT	Gu et al.[21]	https://www.bioconductor.org/packages/release/bioc/html/rGREAT.html
PICS algorithm	Farh et al.[17]	www.broadinstitute.org/pubs/finemapping
PWMscan	Ambrosini et al.[109]	https://ccg.epfl.ch/pwmtools/pwmscan.php
coloc	Giambartolomei et al.[110]	http://coloc.cs.ucl.ac.uk/coloc/
Linkage Disequilibrium Calculator	Ensembl genome database project	https://www.ensembl.org/Homo_sapiens/Tools/LD

EXPERIMENTAL MODEL AND STUDY PARTICIPANT DETAILS

This study was approved by the Ethics Review Committee of Human Research of the University of Tartu, Estonia (protocols 270/T-9, 271/M-35). Informed consent was obtained from all the participants in accordance with the Declaration of Helsinki. Patient demographics are listed in Figure 1A.

METHOD DETAILS

Isolation of CD4$^+$ T cells

30mL of peripheral blood was collected in EDTA tubes from patients with SLE (n=11) and psoriasis (n=15) and from age- and sex-matched healthy donors (n=11 and n=15 respectively) from The University of Tartu, Estonia. PBMCs were obtained by Ficoll Paque (GE Healthcare) density gradient centrifugation. CD4$^+$ T cells were collected by magnetic isolation using CD4 MicroBeads (Miltenyi) on the AutoMACs (Miltenyi) according to the manufacturer's instructions. For CRISPRi experiments, frozen healthy donor naive CD4$^+$ T cells were obtained from AllCells.

H3K27ac ChIP-seq protocol

1 million isolated CD4$^+$ T cells were cross-linked with an 11% formaldehyde buffer, lysed and subjected to sonication using a Bioruptor sonicator UCD-200 (Diagenode) to obtain chromatin fragments of 100–500 bp. Sheared chromatin was immunoprecipitated with 2 μL of anti-H3K27ac antibody (Abcam, ab4729) and 2 μL of Dynabeads M-280 magnetic beads (Sheep Anti-Mouse IgG, Sheep Anti-Rabbit IgG, Invitrogen) using the SX-8G IP-Star Automated System (Diagenode). ChIP samples were decrosslinked at 65°C for 4 hours. After incubation, the samples were treated with 0.2 mg/mL RNaseA (RNase Cocktail Enzyme Mix, Ambion, Life Technologies) and 0.4 mg/mL Proteinase K (Thermo Scientific). DNA was purified with the MinElute PCR Purification Kit (Qiagen) according to the manufacturer's protocol. Sequencing libraries were prepared using the NEBNext Ultra II DNA Library Prep Kit (New England Biolabs) for Illumina according to the manufacturer's instructions. Library quality and concentration were determined using an Agilent Bioanalyzer DNA1000 chip according to the manufacturer's instructions. After passing quality control, libraries were sequenced on an Illumina NextSeq 500 (75-bp single-end mode).

CRISPRi in CD4$^+$ T cells

Individual gRNAs (4 per enhancer, 2 for CD4 promoter and 2 non-targeting scrambled gRNAs, Table S4), were cloned into the CROP-seq Puro-F+E plasmid, containing the optimised F+E tracrRNA sequence[111], using restriction ligation as previously described.[112]

Lentivirus was produced in LentiX HEK293T cells (Takara). Cells were grown to 65–75% confluency prior to transfection. Lentiviral packaging vectors pMD2.G (Addgene 12259) and psPAX2 (Addgene 12260) were combined with CROPseq-Puro-F+E plasmid (containing the sgRNAs) or dCas9-mCherry-ZIM3-KRAB plasmid (Addgene 154473) and transfected using Lipofectamine^{TM} 3000 (Invitrogen). After 6 hours, the transfection medium was replaced with a complete medium supplemented with 1:500 Viralboost reagent (Alstem). Supernatant containing viral particles was harvested after 2 and 3 days and concentrated 100x using Lenti-X concentrator (Takara) following manufacturers instructions.

For T cell transduction, frozen healthy donor naive CD4$^+$ T cells were thawed, cultured and activated using Human T-Activator CD3/CD28 Dynabeads^{TM} (Gibco). The following day, cells were infected with dCas9-mCherry-ZIM3-KRAB lentivirus and the next day with gRNA lentivirus. Cells were selected for gRNA expression using Puromycin and were subsequently reactivated. After three days of reactivation, mCherry positive T cells expressing the dCas9-ZIM3-KRAB protein were sorted by fluorescence-activated cell sorting (FACS) on a BD FACSAria^{TM} Fusion, selecting for viable cells using DRAQ7^{TM} Dye (Biostatus). Sorted cells were immediately lysed in RLT plus buffer (Qiagen) supplemented with 2-Mercaptoethanol.

The CRISPRi effect on predicted enhancer–target genes was measured using quantitative PCR. Briefly, RNA was isolated using the RNeasy mini kit (Qiagen) according to the manufacturer's instructions. RNA concentration was measured using the Qubit^{TM} RNA Broad Range assay kit (Invitrogen), and reverse transcription was performed using SuperScript IV according to the manufacturer's instructions. qPCR was performed with SYBR-Green PCR master mix (Applied Biosystems), and data was processed using the $-\Delta\Delta$Ct method, normalised to the housekeeping gene GAPDH. Primer sequences can be found in Table S9.

QUANTIFICATION AND STATISTICAL ANALYSIS

P-values have been calculated using Fisher's exact test or T-test as indicated in the figure legends.

Processing of publicly available H3K27ac ChIP-seq data

We downloaded H3K27ac data from GEO (GSE71957 for Graves' disease[19] and GSE71595 & GSE71596 for JIA[20]) and processed them as described below.

ChIP-seq pipeline

Reads were trimmed using Trimmomatic v0.36 for illumina TruSeq3-SE adaptors. FASTQC was performed on samples before and after trimming and those samples which passed quality control were used for alignment. The ChIP-seq reads were then aligned to human genome assembly hg38 using Bowtie2[102] with default parameters in "*—very-sensitive*" mode. Aligned reads mapping to ChrM, other unassembled contigs and also reads with minimum mapping quality score < 10 were filtered out using SAMtools v1.5.[103] Additionally, duplicates were removed using Picard tool v2.17.6 using the "*MarkDuplicates"* function.

Peak calling was done per sample using MACS2[104] v.2.0.1 using default parameters and "*–keep-dup all*". Consensus peaks for the samples within each disease were generated with the DiffBind Bioconductor R package using the "*dba.peakset*" function with the requirement that the peaks are present in at least two samples in case of Graves' and JIA and at least three samples in case of Psoriasis and SLE. A consensus peak set for all the diseases together (Psoriasis, SLE, Graves' and JIA) was generated with the peaks present in at least three samples.

The raw counts for the resulting consensus peak sets were generated using the "*dba.count*" function with default parameters.

RNA-seq pipeline

Reads were trimmed using Trimmomatic[101] v0.36 for Illumina TruSeq3-PE-2 adaptors. FastQC was performed on samples before and after trimming and those samples which passed quality control were used for alignment. The reads were then aligned to human genome assembly hg38 using STAR[105] v2.6.0 with default parameters. Aligned reads which were uniquely mapped and in correct pairs were retained. Gene counts were obtained using the "*summarizeOverlaps*" function from the GenomicAlignments Bioconductor R package[106], using the gencode.v28 primary assembly annotation gtf file.

Differential peak/gene analysis

PCA and hierarchical clustering were performed on transformed read counts (regularized log transformation) for peaks/genes in case of ChIP-seq and RNA-seq respectively. This was done as a quality control measure to identify sample similarity based on conditions and to detect any kind of batch effects prior to performing differential peak/gene analysis. Differential analysis for peaks/genes were carried out using the DESeq2 Bioconductor R package[107] with default settings and using the following generalized linear model: "$\sim$ *Age* + *Batch* + *Condition*", where the conditions were patients versus healthy controls for SLE, Graves' disease and psoriasis, and patient SF versus patient PBMCs for JIA. Peaks and genes with an adjusted p-value threshold <= 0.05 were considered significant.

Differential TF activity

Differential TF activity between autoimmune patients and healthy controls for for SLE, Graves' disease and psoriasis, and patient SF versus patient PBMCs for JIA, was estimated using the diffTF tool[27] in analytical mode with default parameters and using HOCOMOCOv11 motifs (as part of the DiffTF workflow). TFs with an adjusted p-value <=0.05 were considered significantly differential. "Briefly, diffTF quantifies the log2-fold change between two conditions (here: patients vs controls) of all peaks and bins peaks based on their GC content. For each TF it splits peaks in each bin into a foreground (peak with TF binding site) and background (peaks without TF binding). Differential TF activity is quantified as the difference in mean between foreground and background. Significance is calculated based on a local FDR procedure (details in[27]).

GWAS-SNPs for autoimmune diseases

The summary statistics for genome-wide association studies for ADs including psoriasis[113], SLE[114], IBD[115], RA[116], celiac disease[85], and asthma[117] were downloaded from NHGRI-EBI GWAS-catalog[54] for the hg38 genome build.

SNPs with p-value < 1e-5 and those mapping not in the MHC region (ch6:20,000,000 – 40,000,000) were selected. These selected GWAS-SNPs together with their linkage disequilibrium (LD) variants, obtained for the hg38 genome build, were used in this analysis. These LD variants were identified using a window of 200kbp and R squared value equal or greater than 0.8 (R2 >= 0.8) around selected GWAS-SNPs used as lead SNP using the LD calculator from https://www.ensembl.org/Homo_sapiens/Tools/LD.

Colocalization analysis of hQTLs and GWAS-SNPs

We used coloc v2.3.1[110] to perform colocalization between hQTLs from naive T cells and GWAS-SNPs belonging to several ADs using their summary statistics as stated above. The hQTL data was obtained from blueprint consortium.

Colocalisation was performed on 400kb regions centered on significant hQTL peaks (p-value < 0.05). In this region, we ran colocalization tests if the number of shared hQTLs and non HLA-GWAS SNPs were greater than 10 (shared SNPs > 10 in 400 kb region). We considered a true colocalization signal, if the probability of association between GWAS-SNP and hQTL due to a shared causal variant given as PP.H4 by coloc, was greater than or equal to 0.8 (PP.H4 >= 0.8).

Generation of naive CD4 T-cell eGRN

We obtained paired RNA-seq and H3K27ac ChIP-seq data from naive $CD4^+$ T cells from 138 healthy donors from the Blueprint consortium to generate eGRN. Both datasets were downloaded from the EGA archive (EGAD00001002671, EGAD00001002673) and processed using ChIP-seq and RNA-seq analysis pipeline as described above. It is based on covariation between enhancer signal

and RNA-expression across individuals, adapted from the workflow described in[51]. The eGRN generation consist of two main steps:

Generation of TF-enhancer links

We obtained putative TF binding sites using PWMscan[109] for all the TFs for which the motif is available from HOCOMOCO v.11. [100] Next, we identified the TF binding sites which overlapped the consensus H3K27ac ChIP-Seq peak set (generated as described above). We then generated a correlation matrix between TFs (columns) and H3K27ac peaks (rows). Each cell in the matrix is a Pearson correlation coefficient between TF expression and H3K27ac signal across all 138 individuals for the corresponding TF-peak pair. We then calculate FDR for each TF-enhancer pair as described in [53] . We used an FDR threshold of 20% for all TFs to define significant TF-enhancer links.

Generation of enhancer-gene links

Enhancers were linked to all the genes within a distance of +/- 250kb TSS and which show positive and significant Pearson correlation coefficient between H3K27ac signal and gene expression across all 138 individuals with an adjusted P-value cutoff of 0.05.

Next, we combined the two steps above which resulted in the generation of a tripartite eGRN containing TF-enhancer-gene links.

Additionally, we include SNP-enhancer-gene links by overlapping known AD SNPs obtained from NHGRI-EBI GWAS-catalogue as described above with the enhancers included in the consensus peak set and correlating these enhancers to putative downstream target genes as described in step 2. Similarly, as above, we also include Differentially acetylated-enhancer-gene links by overlapping differentially acetylated enhancers (AD patient vs controls) with consensus enhancer peaks.

Generation and pruning of AD specific eGRNs

The autoimmune eGRNs for each disease (Graves' disease, SLE, JIA and psoriasis) were generated separately. Each of these disease-specific eGRNs involved filtering the naive $CD4^+$ T cell eGRN. We retained genes connected to at least two upstream nodes (TFs or peaks) that are linked with different or the same types of disease specific molecular evidence. These molecular evidences include (i) differentially active TFs, in which case we would keep their regulatory elements and target genes, (ii) differentially acetylated enhancers, in which case we would keep their upstream linked TF and their downstream linked target gene. In addition, we keep enhancers and their linked TF and target genes if (iii) the enhancer overlaps with a GWAS-SNP of the corresponding disease, or (iv) if enhancer overlaps with with naive T cells peaks associated with significant colocalized histone quantitative trait loci (hQTLs) -AD GWAS SNPs

We applied additional criteria to this filtered network. Specifically, a gene is kept if any of the following is true:

a. It is connected to more than one differentially active TF with their regulatory activities going in the same direction (either upregulation or downregulation).
b. It is connected to more than one differential H3K27ac peak with their activity going in the same direction (either upregulation or downregulation)
c. It is connected to a differentially active TF AND a differentially active peak with their regulatory activities in the same direction
d. It is connected to a regulatory element with overlapping GWAS-SNPs/colocalized signal

Generation and pruning of the general AD eGRN

The general AD eGRN was generated by filtering the naive $CD4^+$ T cell eGRN in a similar way as described above but with upstream nodes (TFs, peaks) that are linked to any molecular disease evidence (differentially active TFs, differentially acetylated enhancers, GWAS-SNPs, (hQTLs) -AD GWAS SNPs peaks) but coming from at least two diseases. Specifically, a gene is kept if any of the following are true:

(1) It is connected to at least 2 TFs that is shared between at least 3 diseases (SLE, JIA, Psoriasis and Grave's disease) AND that go in the same direction within at least one of the shared disease / 1 TF that is shared between at least 3 diseases (SLE, JIA, Psoriasis and Grave's disease) AND that go in the same direction across the shared diseases
(2) It is connected to at least two differential peaks that are shared between at least two diseases (SLE, JIA, Psoriasis and Grave's disease) AND that go in the same direction across the shared diseases
(3) It is connected to a peak that overlaps/is colocalized with a GWAS-SNPs associated with any one of ADs like Graves' disease, Psoriasis, SLE, JIA, Celiac, RA, IBD and Asthma AND either a differentially active TF or peak in any of the disease covering at least two

Prioritisation of genes from autoimmune disease networks

The genes from all AD eGRNs were prioritised first based on i) number of types of molecular disease evidence followed by ii) total number of molecular evidences. Genes are given the same priority if they have the same type and total number of molecular evidences.

For the identification of the top shared genes among different AD eGRNs, they were first selected if they were shared between 3 or more AD eGRNs. Next, they were prioritised based on following factors in the sequential order i) the number of AD eGRNs they are part of ii) the number of molecular disease evidence types and iii) the total number of molecular evidences. To further refine the list of

prioritised genes, we used three additional metrics i) regulation by a fine mapped autoimmune disease variant ii) significant change in gene expression upon T cell stimulation iii) annotation from known association to autoimmune condition.[56]

Publicly available epigenetic data for Graves and JIA

H3K27ac ChIP-seq data from PBMC derived $CD4^+$ T cells belonging from healthy controls and Graves' disease patients was obtained from the NCBI gene expression omnibus using accession code GSE71957.[19] H3K27ac ChIP-seq data for $CD4^+$ T-cell from peripheral blood and synovial fluid from JIA patients and peripheral blood from three healthy donors was obtained using the accession code GSE71596.[20] All samples were processed using the ChIP-seq pipeline as discussed above and used for further analysis in our study.

Gene Ontology (GO) and GREAT enrichment analysis

The GO enrichment analysis for genes present in disease-specific and general AD networks were performed using the "*enrichGO*" function from clusterProfiler package Bioconductor R package[108] for biological processes. All the genes in the naive T cell network were used as the background for the enrichment. Terms with an adjusted p-value cutoff <= 0.1 were considered significant.

The nearby genes in different clusters of histone acetylation signal in autoimmune disease were annotated and an enrichment analysis using GO ontology for biological process was performed using rGREAT Bioconductor R package[21] under default settings with hg38 genome assembly. The consensus H3K27ac peak set which was used for generating clusters was used as background for calculating the enrichment. Terms with an adjusted p-value cutoff <= 0.1 were considered significant.

Drug target enrichment

A combined list of drug targets for autoimmune diseases under consideration including psoriasis, SLE, Graves' disease, JIA, Celiac disease, IBD, and asthma was generated. The drug targets were downloaded separately for each disease from the open targets platform https://www.targetvalidation.org/. The genes in the AD eGRNs (general plus disease-specific networks together) were tested for drug target enrichment against all the genes present in the naive $CD4^+$ T cell network as a background using the "*fisher.test*" base function in R. Enrichments with Fisher's exact test p-value <=0.05 were considered significant.

Fine mapped GWAS-SNPs

Fine-mapped GWAS variants for ADs were generated using the probabilistic identification of causal SNPs (PICS) algorithm.[17] AD variants were downloaded from i) a previously published list [17] and lifted to the hg38 genome build and ii) the PICS data portal under the filename "PICS2-GWAScat-2020-05-22.txt.gz" from https://pics2.ucsf.edu for the hg38 genome build. PICS probability of >50% was used to filter the variants. We identified target genes by overlapping these variants with the peaks from the naive T cell eGRN and then used the peak-gene link from this eGRN to assign the target genes.

Stimulation landscape in CD4+T cells

ATAC-seq and RNA-seq data for $CD4^+$ T cell subtypes belonging to Tfh, Th17, Treg, Th1 and Th2 for resting and stimulated conditions were obtained from the NCBI gene expression omnibus using accession codes GSE118189 and GSE118165 respectively.[58] These samples were then processed using ATAC-seq pipeline and RNA-seq pipeline followed by differential peak/gene analysis between stimulation and resting conditions using DESeq2[107] as described above. We defined stimulation-responsive genes in these cell subtypes as those that are significantly differentially expressed between stimulation and resting cells using DESeq2 with p-adjusted<= 0.1.